

TI Designs: TIDA-01524

汽车高效率电源前端和多相处理器电源参考设计



说明

此处理器电源参考设计是一种汽车电源解决方案，可用于支持高级驾驶员辅助系统 (ADAS) 中的高性能单核电压应用处理器。此设计可支持高达 10A 的核心电源电流（电压为 0.9V）。此外还可在宽输入电压范围内工作，能够应对电池反向情况，支持低至 3.5V 输入的启停和冷启动操作，并产生不受干扰的输出。与具有较快开关频率的电源前端相比，此电源前端的 sub-AM 波段开关频率可提高效率并降低电路板温度。多相电源配置和集成有助于降低电磁干扰 (EMI) 和提高效率。此参考设计还提供了 CISPR 25 5 类传导发射测试结果。

资源

TIDA-01524	设计文件夹
LP87561-Q1	产品文件夹
LMS3655-Q1	产品文件夹
LM26420-Q1	产品文件夹
LM74700-Q1	产品文件夹
LM2775	产品文件夹
TIDA-00530	产品文件夹
TIDA-00699	产品文件夹
PMP7233	产品文件夹
AutoCrankSim-EVM	工具文件夹

特性

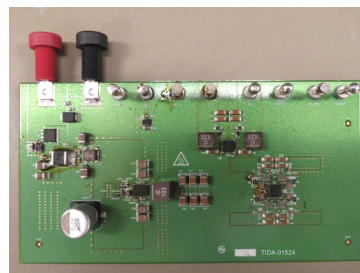
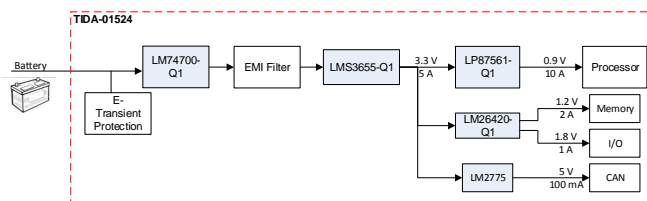
- 具有扩频功能的 5A 集成式 400kHz 同步宽输入电压降压直流/直流转换器
- 为应用处理器的核心电压轨提供 10A 电流（电压为 0.9V）
- 智能二极管反向电池保护功能实现最小压降
- 工作电压范围为 3.5V 至 36V，支持启停和冷启动
- 交错四相核心电压电源可最大限度减小纹波、EMI 和电感器尺寸
- 通过了 CISPR 25 5 类传导发射测试
- 用于 5V CAN 电源的小型开关电源升压转换器降低了解决方案尺寸和 BOM 成本

应用

- [前置摄像头](#)
- [驾驶员监控系统](#)
- [摄像头监控系统](#)
- [环视](#)
- [ADAS 域控制器](#)



咨询我们的 E2E 专家



该 TI 参考设计末尾的重要声明表述了授权使用、知识产权问题和其他重要的免责声明和信息。

1 System Description

Camera-based ADAS systems process and analyze video feeds from local or distributed cameras and either output video or use machine-vision algorithms to perceive the environment in and around the car. Such functions are made possible by application processors, which typically have specific power requirements. Application processors are used in automotive camera systems such as front camera, mirror replacement, driver monitoring, surround view systems, and to some extent, sensor fusion systems. This design focuses on applications up to 15 W and application processors with single-core voltage domains. This design has been created with the following features in mind:

- System efficiency of at least 75% with nominal input voltage
- Provide 10 A at 0.9 V to a single-core voltage rail for video application processors
- Minimize electromagnetic interference (EMI) and solution size with a multiphase configuration for the single-core-voltage rail supply
- Limit conducted emissions below CISPR 25 Class 5 conducted emissions limits
- Withstand reverse battery condition
- Operate through start-stop and cold-crank down to 3.5 V
- Optimize the individual blocks for the smallest possible solution size
- Provide power for CAN PHY and external DDRx memory

图 1 shows an example of a front camera system.

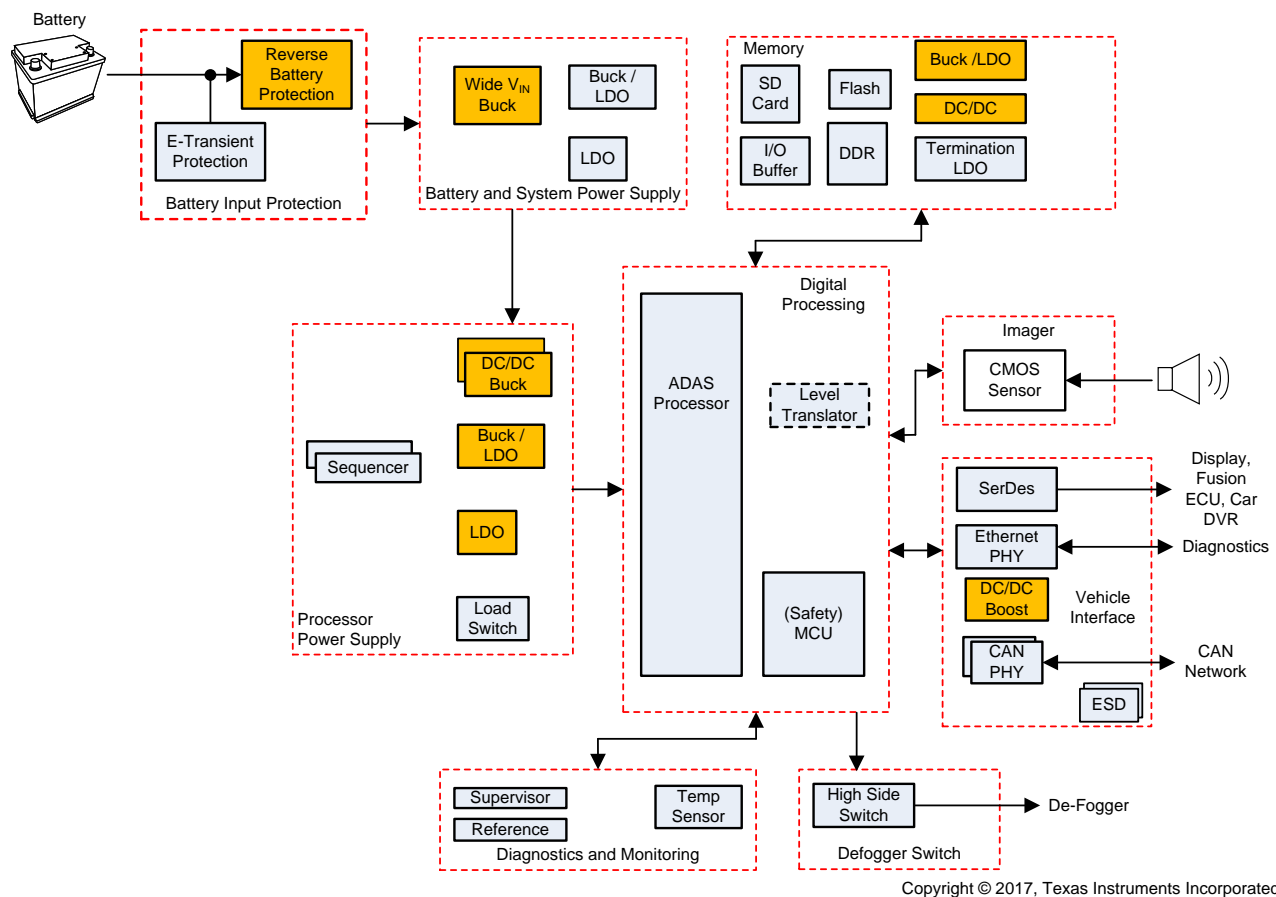


图 1. Example of Front Camera Block Diagram

These camera systems vary in the location of cameras and the number of cameras and processors. The red blocks are all components located on the TIDA-01524 board and which cover the power requirements for an application processor. Functionality, such as voltage supervision and sequencing, are partially integrated into the integrated circuits (ICs). 图 2 shows each subsystem and block on the actual TIDA-01524 board.

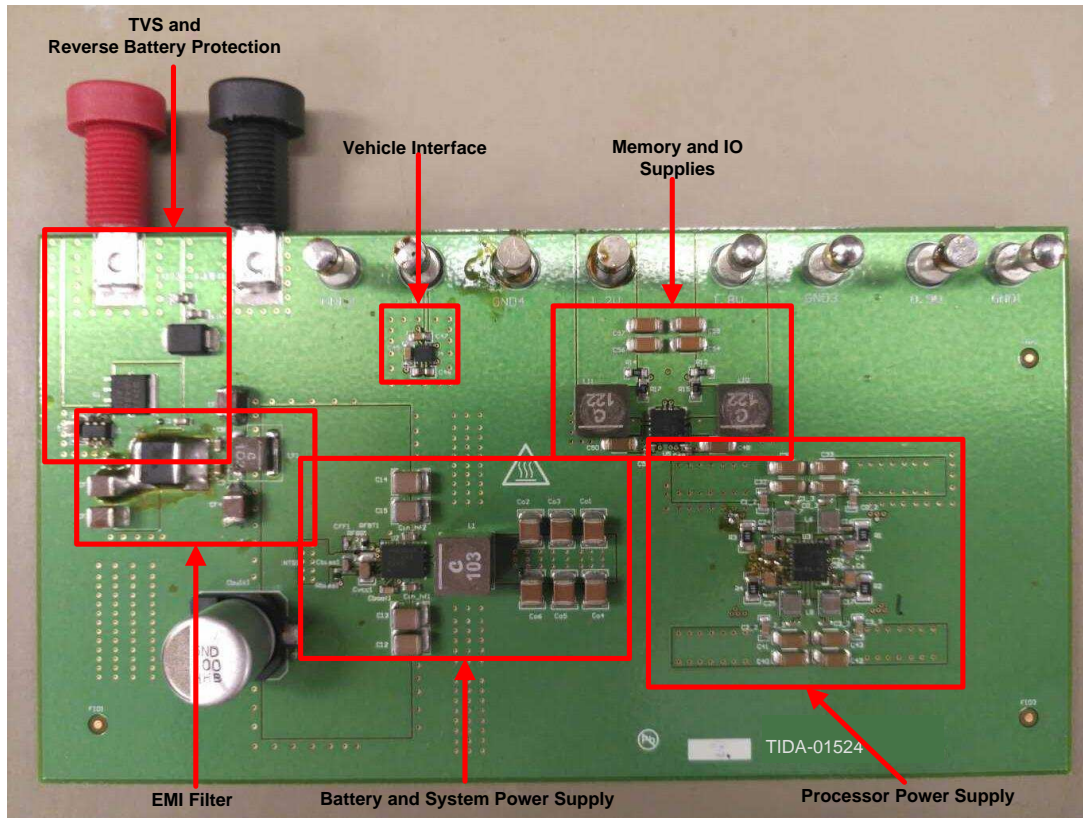


图 2. TIDA-01524 Subsystems Highlight

1.1 Key System Specifications

表 1. Key System Specifications

PARAMETER	COMMENTS	MIN	TYP	MAX	UNIT		
SYSTEM INPUT							
V_{IN}	Input voltage	Battery voltage range (DC)		3.5	13.5	36.0	V
V_{CORE}	Core-voltage supply output voltage	—	0.9	—	—	V	
I_{CORE}	Core-voltage supply output current	—	—	10.0	—	A	
$V_{I/O}$	I/O supply voltage	—	1.8	—	—	V	
$I_{I/O}$	I/O supply output current	—	—	1.0	—	A	
V_{MEMORY}	Memory supply voltage	—	1.2	—	—	V	
I_{MEMORY}	Memory supply output current	—	—	2.0	—	A	
V_{CAN}	CAN supply voltage	—	5.0	—	—	V	
I_{CAN}	CAN supply output current	—	—	0.1	—	A	

2 System Overview

2.1 Block Diagram

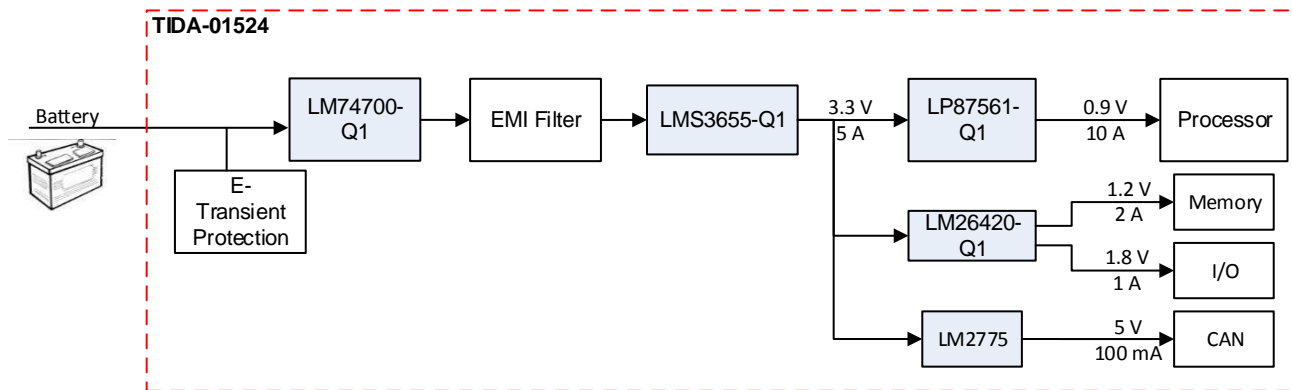


图 3. Power Solution for Single-Core-Voltage Application Processors

2.2 Highlighted Products

This reference design uses the following TI products:

- LMS3655-Q1: 5.5-A, 400-kHz synchronous buck converter with a wide input voltage range from 3.5 V to 36 V and spread spectrum (42-V transients), enabling the device to work directly from an automotive battery
- LP87561-Q1: Four-phase, 16-A buck converter with I²C compatible serial interface designed to meet power management requirements for the latest automotive processor applications
- LM26420-Q1: Highly-efficient, dual, 2-A synchronous buck converter with independent power good and precision enable for each output
- LM2775: Highly-compact, switched-capacitor 5-V boost converter
- LM74700-Q1: The "Always On Smart Diode Controller" is a high-side N-channel field-effect transistor (N-FET) controller with ultra-low forward voltage drop intended for reverse-battery protection

The following subsections detail each device and explain their selection for this application.

2.2.1 LMS3655-Q1

The LMS3655-Q1 is the main system supply in this reference design. The wide input voltage range, high integration, and excellent efficiency make this device a top choice for the wide-input-voltage power front end. The device switches at 400 kHz, below the AM band (530 kHz to 1.8 MHz). There should be minimal interference in the AM band for all automotive applications. While the external passive components may be larger than for a device with a switching frequency above the AM band, the total efficiency and thermal performance is improved. The LMS3655-Q1 also uses spread spectrum to reduce peaks of the higher harmonics of the switching frequency in the FM band.

The LMS3655-Q1 is designed with a flip-chip or HotRod™ integrated circuit package. This packaging technology drastically reduces the parasitic inductance of pins. As a result, the switch-node waveform shows much less overshoot and ringing. In addition, the layout of the device allows for partial cancellation of current-generated magnetic fields, which reduces the radiated noise generated by the switching action.

Though not used in this reference design, this switcher supports external clock synchronization to avoid beat frequencies between multiple converters or to allow a master to dither the clock signal. This feature can be very useful for optimizing systems for EMI performance.

2.2.2 LP87561-Q1

The LP87561-Q1 contains four step-down DC-DC converter cores that switch at 2 MHz and are configured to a four-phase, single-output configuration to power a single-core voltage rail of an automotive video applications processor with 10 A at 0.9 V. The designer can control and configure the device over the I²C interface. The maximum output current of the device is actually 16 A (4 A per phase); however, the designer must consider thermal limitations.

For application processor power delivery, a multiphase synchronous buck converter offers several advantages over a single power stage converter. The load current in a multiphase converter is shared evenly among interleaved phases, which eases the inductance and saturation current requirements for each output inductor. Less inductance allows for higher dynamic current, which improves transient response and recovery times. An added benefit is that the heat generated is greatly reduced for each channel due to the fact that current is shared between phases.

Although not used in this reference design, the device does have internal sequencing, which can eliminate the requirement for external sequencer ICs, further reducing the solution footprint. This device also supports remote differential voltage sensing, programmable start-up and shutdown delays, using an external clock input for switching, spread-spectrum, and phase interleaving.

2.2.3 LM26420-Q1

The LM26420-Q1 is a dual, 2-A integrated buck regulator providing 2 A at 1.2 V to memory and 1 A at 1.8 V to the I/O voltage in this design. The switching frequency of this device is 2.2 MHz, which is above the AM band. Each output has independent power good and precision enable signals. This design does not have a sequencing requirement, so these signals remain unused.

The 2-A, 1.2-V supply is intended for 1GB of DDR3 memory, which is sufficient for the targeted low-end processing applications and the 1-A, 1.8-V supply provides sufficient headroom for the I/O.

2.2.4 LM2775

The LM2775 is a fixed, 5-V switched capacitor boost converter for CAN PHY. Compared to an inductor-based solution, the switched capacitor approach reduces the total solution size. The device switches above the AM band at 2.0 MHz. Because 5 V at 200 mA is required for a single CAN PHY, this device is optimized for single CAN PHY applications. The package is a very small 2x2-mm WSON. The only required external components are the I/O capacitors and switched capacitor.

The LM2775 has output disable control. When the device is in shutdown, setting the OUTDIS pin high or low pulls the output voltage to GND or leaves the output in a high impedance state.

2.2.5 LM74700-Q1

The LM74700-Q1 is used for low-loss reverse polarity protection. Using a charge pump, this device controls an external N-FET in series with the battery supply input to act as an ideal diode, with a very-low voltage drop and power loss as opposed to a discrete diode solution. This controller is "Always On" to avoid periodic voltage drops at the input. After detecting a reverse-battery condition, the device quickly turns off the field-effect transistor (FET) that isolates and protects the downstream circuitry.

The voltage drop across the FET is negligibly small, which allows for more input voltage headroom for the wide input voltage buck converter, permitting it to operate at even lower battery input voltages. For example, a cold-crank condition occurs when the battery tries to energize the starter of the engine and the battery voltage drops as low as 3.5 V. With a diode solution, the voltage at the input of the buck converter will be 3.5 V minus the typical diode drop of 0.7 V or 2.8 V. This input voltage is too low for the converter to regulate the 3.3-V system voltage. With the smart diode solution, input voltage at the buck will be close to 3.5 V during this condition and will continue to regulate.

2.3 System Design Theory

2.3.1 Printed-Circuit Board (PCB) and Form Factor

This design does not have any specific requirements for the board geometry. The main objective is to have as small of a solution size as possible for each supply. 图 4 shows a three-dimensional (3-D) rendering of the PCB, followed by a labeled photograph of the actual board in 图 5.

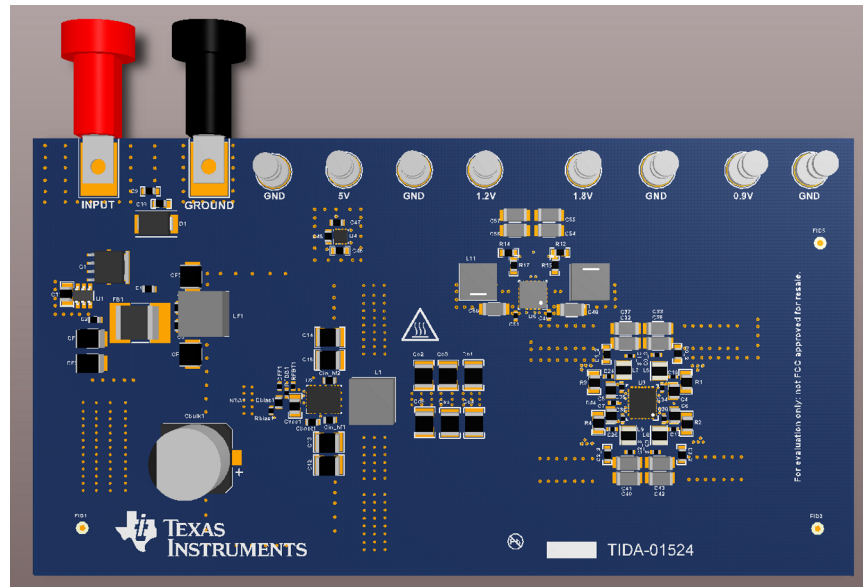


图 4. TIDA-01524 PCB Render

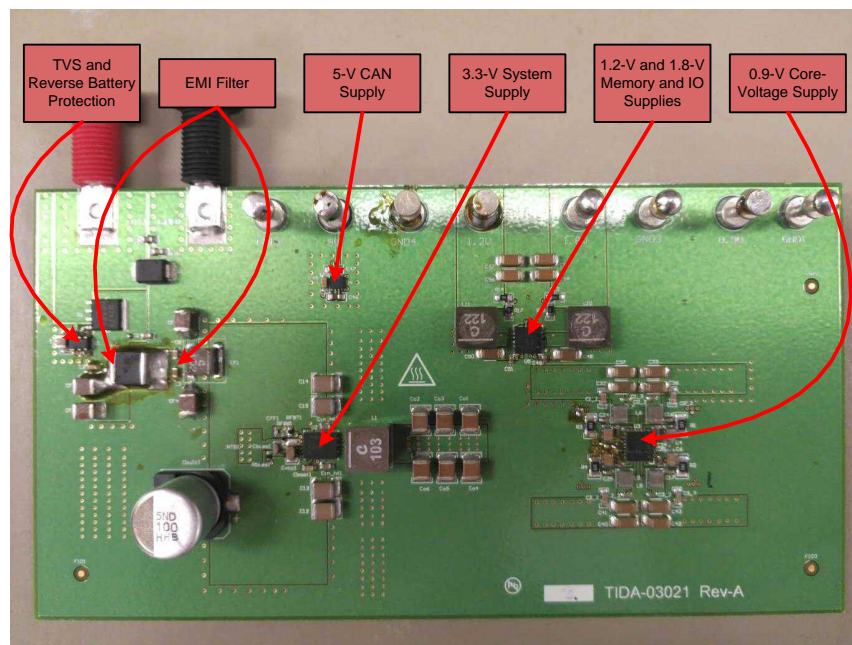


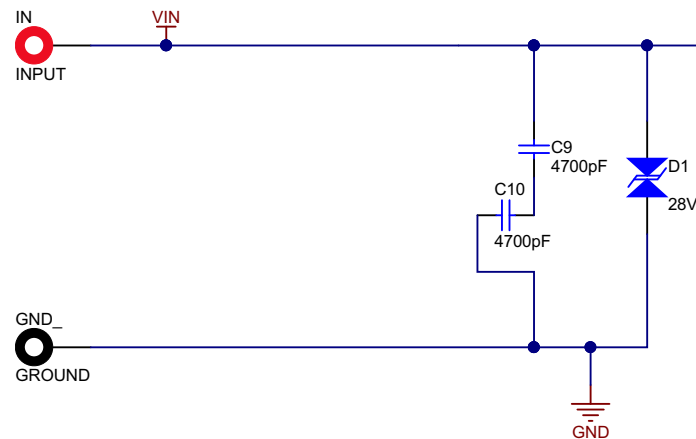
图 5. TIDA-01524 Labeled Supplies and Components

2.3.2 Input Protection and Wide- V_{IN} DC-DC

2.3.2.1 TVS Diodes

Transient voltage suppression (TVS) diodes are required on the supply input of the system to protect against both positive and negative going transients. The transients of concern are detailed in ISO 7637-2:2004, pulses 1 and 2a. Many systems in a car can simply shut down during these transients until the condition passes; alternatively, many ADAS applications require continuous operation. For this reason, the transients must be shunted instead of using an overvoltage shutdown scheme.

图 6 shows a schematic of the input transient protection.



Copyright © 2017, Texas Instruments Incorporated

图 6. Input Transient Protection

The diode breakdown voltages have been chosen such that transients are clamped at voltages that protect the MOSFET and the rest of the system. The positive clamping device must clamp above a double-battery (jump-start) and clamped load dump voltages, but lower than the maximum operating voltage of the downstream devices. In this case, the requirement is to clamp around 28 V but have a maximum clamping voltage below 40 V. Ideally, the best choice is to specify 36 V as the approximate maximum clamping voltage.

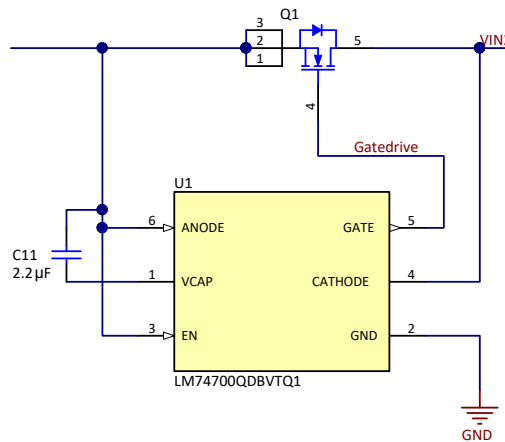
The reverse clamping device must clamp all negative voltages greater than the battery voltage so that it does not short out during a reverse-battery condition.

Due to the energy of the pulses, SMD-sized TVS diodes with 600-W instantaneous peak power ratings are the required minimum specification. This design uses a 600-W, 28-V bidirectional TVS diode.

2.3.2.2 Reverse Battery Protection

Reverse battery protection is a requirement in nearly every electronic subsystem of a vehicle, both by original equipment manufacturer (OEM) standards as well as ISO 16750-2, an international standard that pertains to supply quality.

图 7 shows a schematic of the reverse battery input protection.



Copyright © 2017, Texas Instruments Incorporated

图 7. Reverse Battery Input Protection

Rather than use the traditional diode rectifier solution for reverse battery protection, this implementation uses an N-channel MOSFET driven by the LM74700-Q1 device. The power dissipation of a discrete diode solution is significantly higher due to the typical 600-mV to 700-mV forward drop. A very-low forward voltage drop can be achieved using low $R_{DS(ON)}$ external N-channel MOSFETs. This low forward voltage drop from the supply to the system yields much higher efficiency, less heat, and a lower input voltage operating range while protecting the system from a reverse polarity condition.

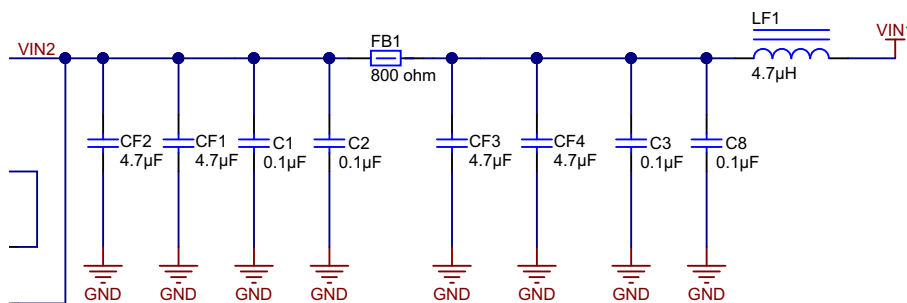
The FET must have a rating which is at least as high as the clamped input voltage. This reference design uses a 40-V N-FET with a 2-V gate-source threshold voltage.

2.3.2.3 Input Capacitors Exposed to Battery Inputs

The final consideration for the front-end protection is the input capacitors. This design uses two, 100-V rated capacitors in series between the battery line and ground, which effectively makes a 200-V rated capacitor of half the nominal capacitance value, to suppress voltage transients detected at the input to protect downstream devices.

2.3.2.4 Input EMI Filter

The schematic in 图 8 shows the EMI filter at the system supply input, after the reverse battery protection.



Copyright © 2017, Texas Instruments Incorporated

图 8. Input EMI Filter Schematic

The inductor LF1 attenuates high-frequency noise coupling back onto the input. Decoupling capacitors C3 and C8 filter out the high-frequency noise that the inductor LF1 cannot attenuate.

The ferrite bead FB1 has a higher resonant frequency than inductor LF1, around 100 MHz. FB1 attenuates unfiltered noise around this 100-MHz band that has been conducted upstream from the LF1-C8 node to VIN2, and increases the impedance for higher-frequency currents that can come from the larger upstream loop, from VIN2 to downstream components after VIN1. Similar to capacitors C3 and C8 after LF1, the decoupling capacitors C1 and C2 provide a low impedance path for high-frequency currents to ground.

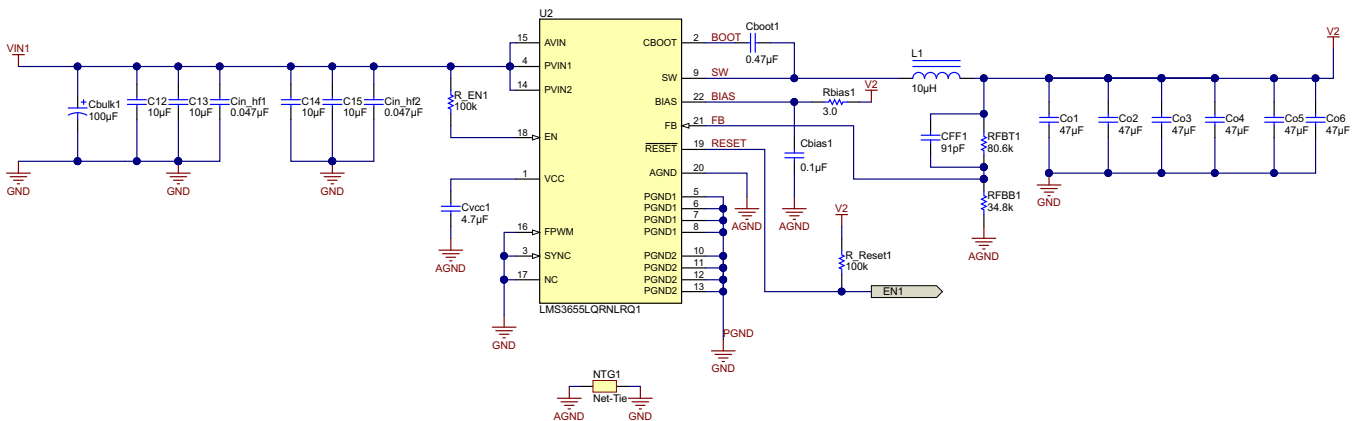
When selecting and adding decoupling capacitors, it may seem attractive to simply add more capacitors. No matter how much decoupling is used, designers must take careful consideration to avoid parallel resonances resulting from the unseen parasitics of the passives. Parallel resonances can cause EMI problems that may be difficult to pinpoint and address.

While it is critical to select the right components for the EMI filter, strategically laying out these components is equally critical for an effective EMI filter.

2.3.2.5 Wide Input Voltage Buck Converter

The LMS3655-Q1 is an AECQ100-qualified, wide-input voltage buck regulator used as a front-end supply to provide a 3.3-V system voltage. With a nominal input voltage range of 3.5 V to 36 V and transients up to 42 V, the device can continue operation through most battery conditions such as start-stop, cold-crank, and load dump.

图 9 shows a schematic of the wide input voltage buck.



Copyright © 2017, Texas Instruments Incorporated

图 9. Wide Input Voltage Buck

The LMS3655-Q1 delivers 5 A at a 400-kHz switching frequency in the above configuration. This setup configures the device for automatic light load mode, which means that the device moves between pulse-frequency modulation (PFM) and pulse-width modulation (PWM) mode as the load current changes. This device has spread spectrum enabled. As the switching frequency operation is below the AM band, automatic shift into PFM mode is acceptable because the switching frequency is still below the AM band and not inside the band.

2.3.3 Power Supply Design Considerations

For this power supply, choose inductors such that:

- The ripple current is between 20% to 40% of the load current I_{LOAD} with the given switching frequency, input voltage, and output voltage. This reference design uses 40%.
- The temperature ratings are appropriate for automotive applications, typically -40°C to 125°C for ADAS applications.
- Saturation current is chosen per 公式 1 for peak current, plus additional margin.

$$I_{SAT} (I_{LOAD} + 0.5 \times I_{RIPPLE}) \times 1.2 \quad (1)$$

An important recommendation for ADAS applications is selecting ceramic capacitors that use X7R dielectric material, which ensures minimum capacitance variation over the full temperature range. The voltage rating of the capacitors must be greater than the maximum voltage and twice the typical voltage across its terminals to avoid DC bias effects. The amount of output capacitance used depends on output ripple and transient response requirements, for which there are many equations and tools available online to help estimate. The supplies in this solution have been designed for a $\pm 2.5\%$ total transient response. Low equivalent series resistance (ESR) ceramic capacitors have been used exclusively for the purpose of reducing ripple. For internally-compensated supplies, see the device-specific data sheets, as they may have limitations on acceptable LC output filter values.

ICs must always be qualified per AECQ100. TI parts that are qualified typically have part numbers ending in "-Q1".

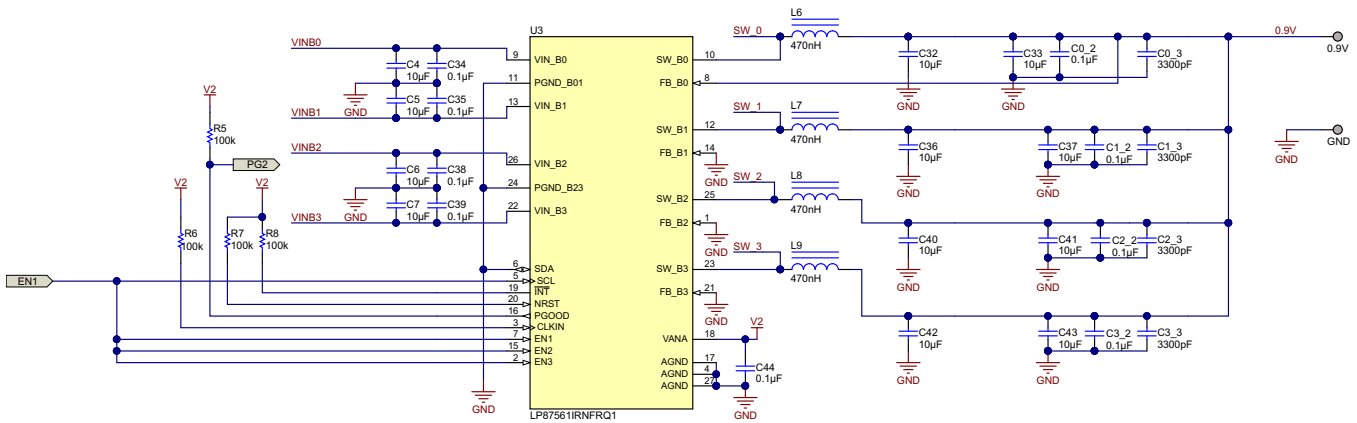
For improved accuracy, all feedback resistor dividers must use components with 1% tolerance.

2.3.3.1 LP87561-Q1 Core-Voltage Supply

The LP87561-Q1 is a four-phase single output device. Rather than using external resistor dividers to set core configurations, operating modes, slew rates, and status signal delays, the device is configurable through an I²C interface. In this design, the I²C lines are unused and the device runs in the default state. The default values of key device parameters are defined as follows:

- $V_{OUT} = 0.9\text{ V}$
- Forced PWM mode
- Automatic phase adding and shedding
- Switch current limit = 5 A
- Output voltage slew rate = 10 mV/ μs
- Start-up delay = 0 ms
- Shutdown delay = 0 ms

图 10 shows the schematic for the device.



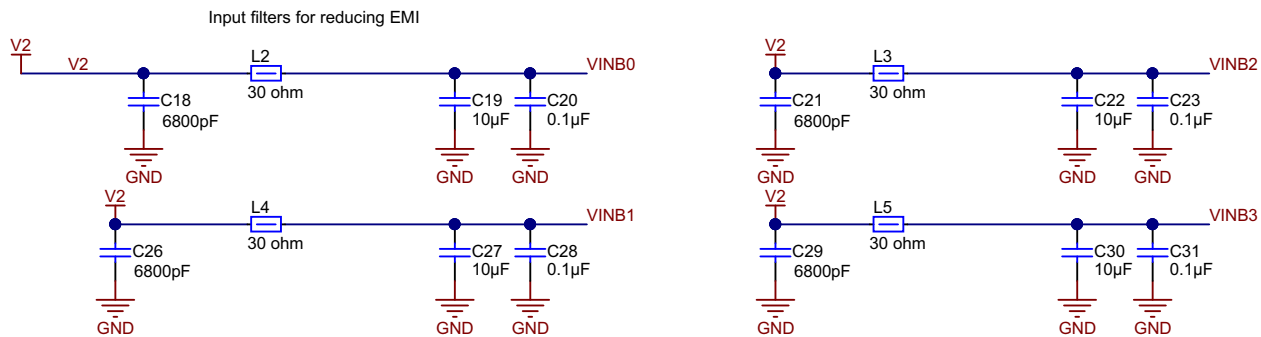
Copyright © 2016, Texas Instruments Incorporated

图 10. Core-Voltage Supply Schematic

For more detail on the design procedure and component selection, see [LP87561F-Q1 Four-Phase 16-A Buck Converter With Integrated Switches \(SNVSAS3\)](#). The following subsections describe the input EMI filters and snubber circuits for each phase.

2.3.3.1.1 LP87561-Q1 Input EMI Filter

图 11 shows the schematic for the EMI filter for each phase input.



Copyright © 2017, Texas Instruments Incorporated

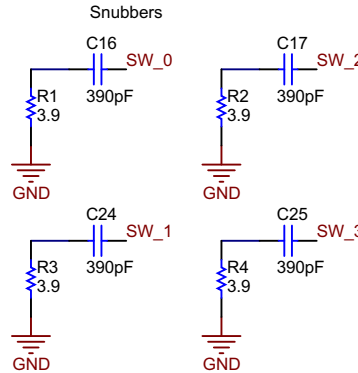
图 11. Input EMI Filter for Each Phase

These input EMI filters are pi filters. Similar to the system input EMI filter that addresses, the ferrite bead acts as both an AC current-loop choke from a larger upstream loop and an attenuator of high-frequency noise conducted back into the system. A 30-Ω ferrite bead is selected for low DC resistance (DCR) and because 30 Ω at 100 MHz is a good starting point for optimization. This impedance is not required to be very high, but just high enough for high-frequency currents to flow through lower impedance paths through the decoupling capacitors, forming a tighter loop with the supply input and output. The 6800-µF capacitor provides a low-impedance path to ground for the very-high-frequency noise conducted back into the system that has not been suppressed by the ferrite bead.

The selected component values are based on commonly-used and suggested values and are simply intended to serve as a good starting point. Component value optimization is empirical. The layout of these components is just as important as the component values. A bad layout can make a thoroughly designed filter schematic useless or even introduce problems into the circuit.

2.3.3.1.2 LP87561-Q1 Snubber Circuits

Switch node ringing can cause problems for a device or system. Here, the main concern is that the switch node does not create EMI problems. This addressed by using a snubber circuit. 图 12 shows the schematic of the snubber circuit for each phase output.



Copyright © 2017, Texas Instruments Incorporated

图 12. Output Snubber Circuit for Each Phase

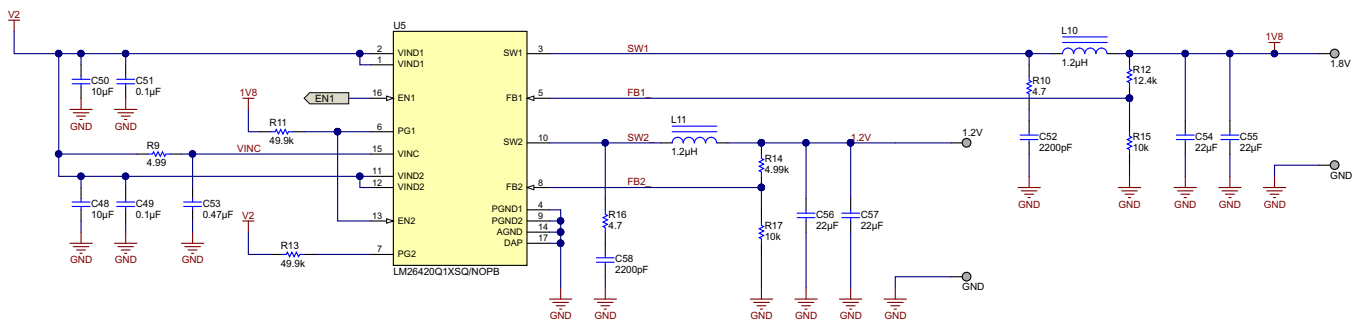
The snubber circuit reduces switch node ringing at an efficiency cost by filtering out the higher frequencies (> 100 MHz) due to the high dv/dt at the switch node.

Just as for the device input EMI filter, component values have been selected based on commonly-used and suggested values and are simply intended to serve as a good starting point. Component value optimization is empirical. The layout of these components is just as important as the component values. A bad layout can make a thoroughly-designed filter schematic useless or even introduce problems into the circuit.

2.3.3.2 LM26420-Q1 Memory and I/O Supply

The switching frequency of the LM26420-Q1 is preset to 2.2 MHz, which reduces the size of output inductors and maintains a small total solution size. The current mode architecture of the IC simplifies the regulator compensation, reducing design time and requiring fewer external components than voltage mode regulators. The device output voltage regulation uses current-mode control, which provides fast transient response. The device is internally compensated, which further reduces the total solution size.

图 13 shows the memory and I/O supply schematic.



Copyright © 2017, Texas Instruments Incorporated

图 13. Memory and I/O Supply Schematic

For more detail on the design procedure and component selection, see [LM26420/LM26420-Q0/Q1 Dual 2-A Automotive-Qualified, High-Efficiency Synchronous DC-DC Converter](#) (SNVS579).

2.3.3.3 LM2775 5-V CAN Supply

The LM2775 device provides the 5-V output voltage required for a CAN bus (see [图 14](#)).

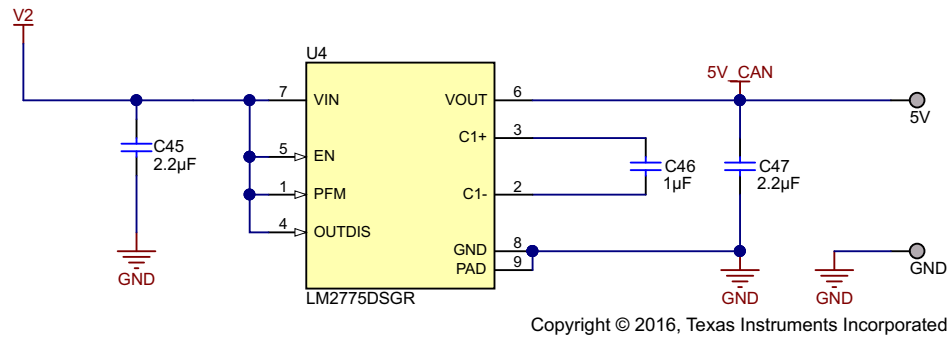


图 14. 5-V CAN Supply Schematic

For more details on the device, see [LM2775 Switched Capacitor 5-V Boost Converter](#) (SNVSA57).

3 Getting Started Hardware

3.1 Hardware

To get started with the TIDA-01524 board, simply connect the leads to the banana jack on the top-left corner of the board. The screw terminals are labeled IN and GND to indicate the correct polarity of the supply (see [图 15](#)).

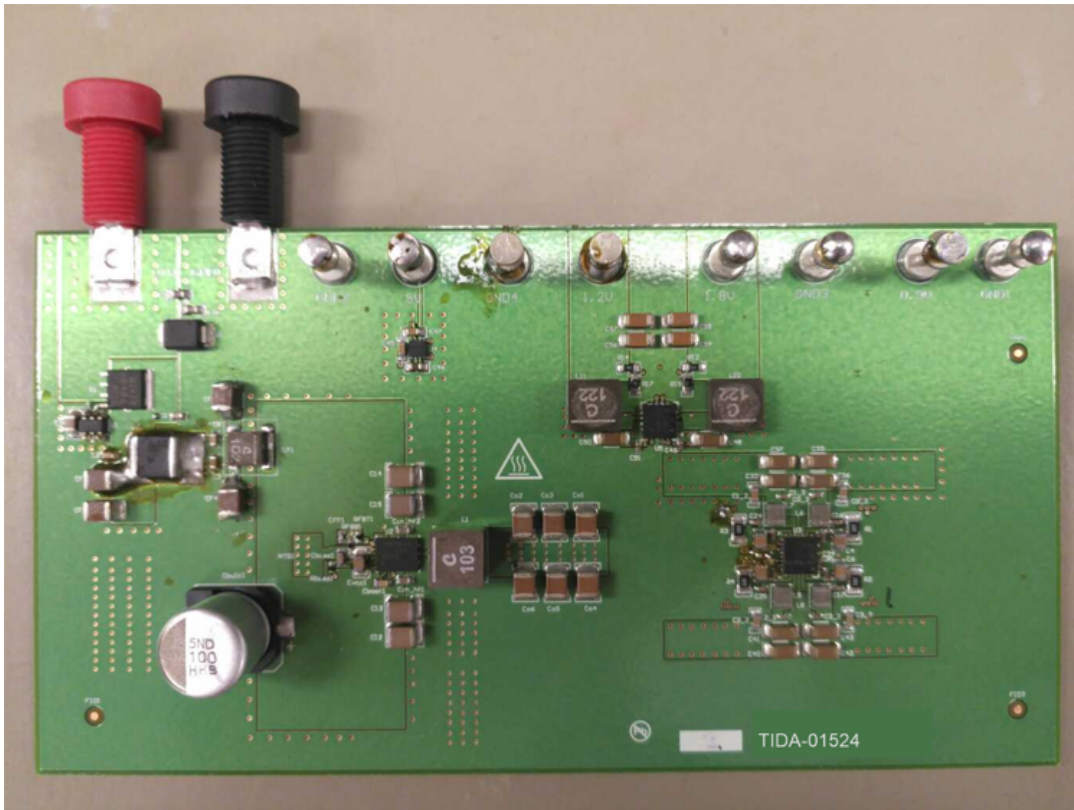


图 15. Board Input Terminals

Connect a power supply that is capable of at least 13.5 V and 2 A to the leads to supply the power.

4 Testing and Results

The following information shows how to set up for the various tests performed on this design.

To perform pulse testing, this design used the AutoCrankSim-EVM: Simulator for Automotive Cranking Pulses Evaluation Module Board. This board is available for purchase at: [AUTOCRANKSIM_EVM: Simulator for Automotive Cranking Pulses Evaluation Module Board](#). If the designer wishes to build the board or simply view the design files, use the power design files from: [PMP7233 Cranking Simulator Reference Design for Automotive Applications](#).

4.1 Test Data

The following subsections show the test data from characterizing the switching power supplies in the system.

4.1.1 Load Regulation and Efficiency

This section presents and discusses the core-voltage supply load regulation and two-stage efficiency test results. 图 16 shows the output voltage variation of the 0.9-V core-voltage supply with varying load current, from no load to full load.

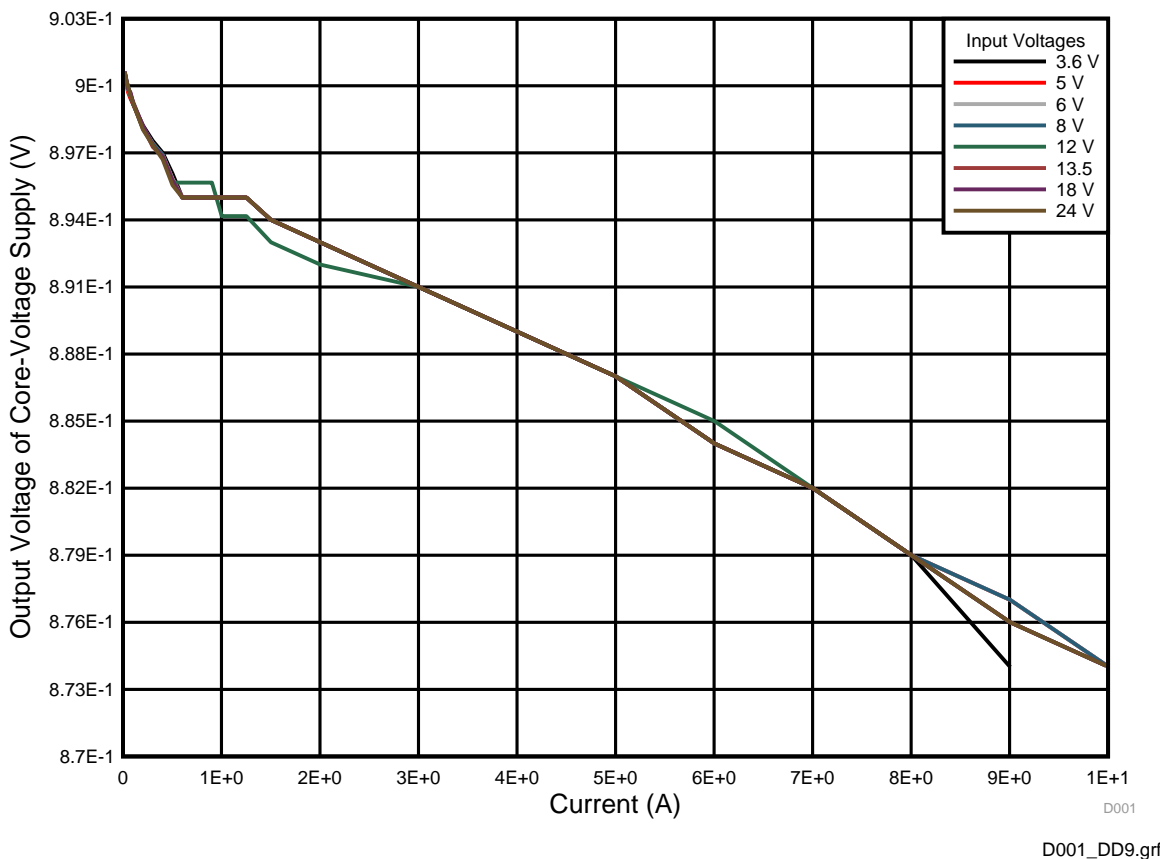


图 16. Load Regulation of Core-Voltage Supply

A close examination of the previous 图 16 shows that the maximum measured deviation from the nominal output of the 0.9-V supply is 2.889%. This value comes from estimating the measured output voltage to be 0.874 V at the full load and nominal input voltage.

The following [图 17](#) shows the efficiency of the two-stage conversion (3.3 V to 0.9 V) used in this design. The two-stage approach consists of the LMS3655-Q1 main 3.3-V system supply feeding the LP87561-Q1 core-voltage supply for the application processor. The core-voltage load current was varied from no load to full load for certain input voltages from 3.5 V to 24 V. This graph plots the data linearly for both x- and y-axes.

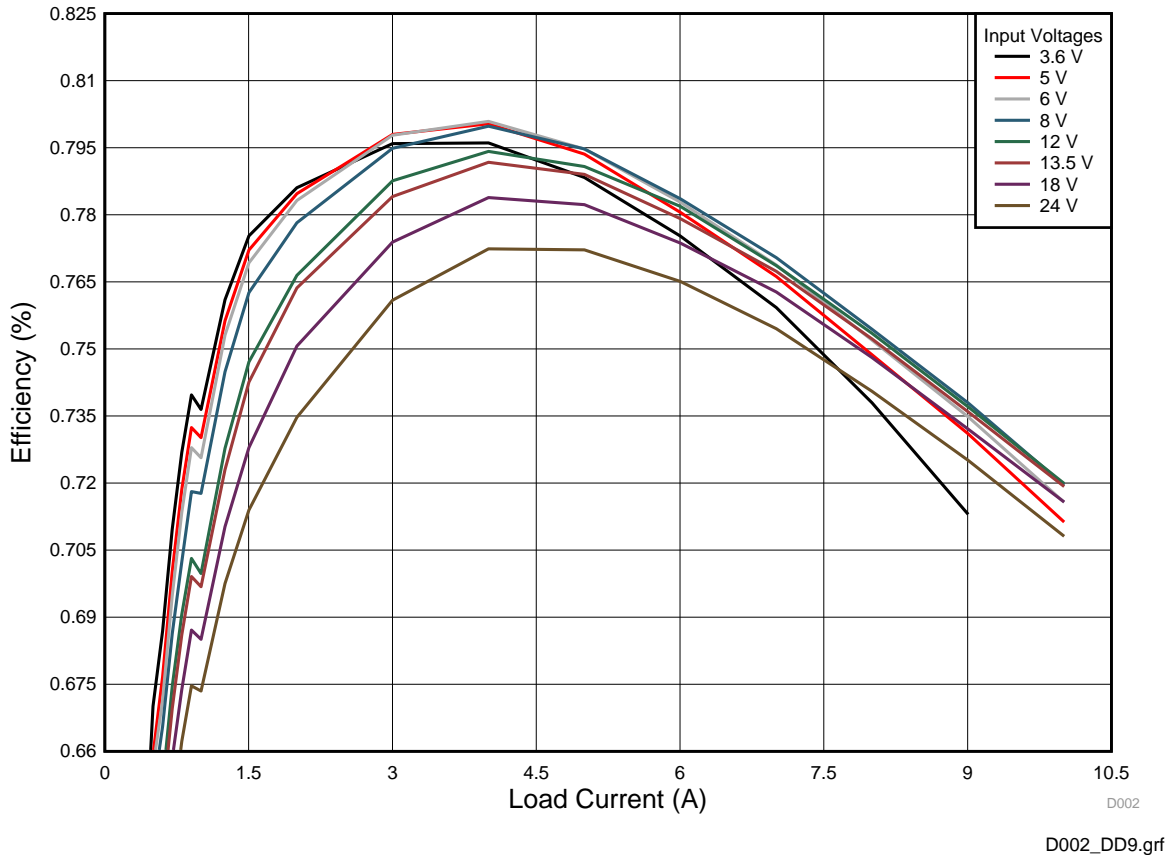
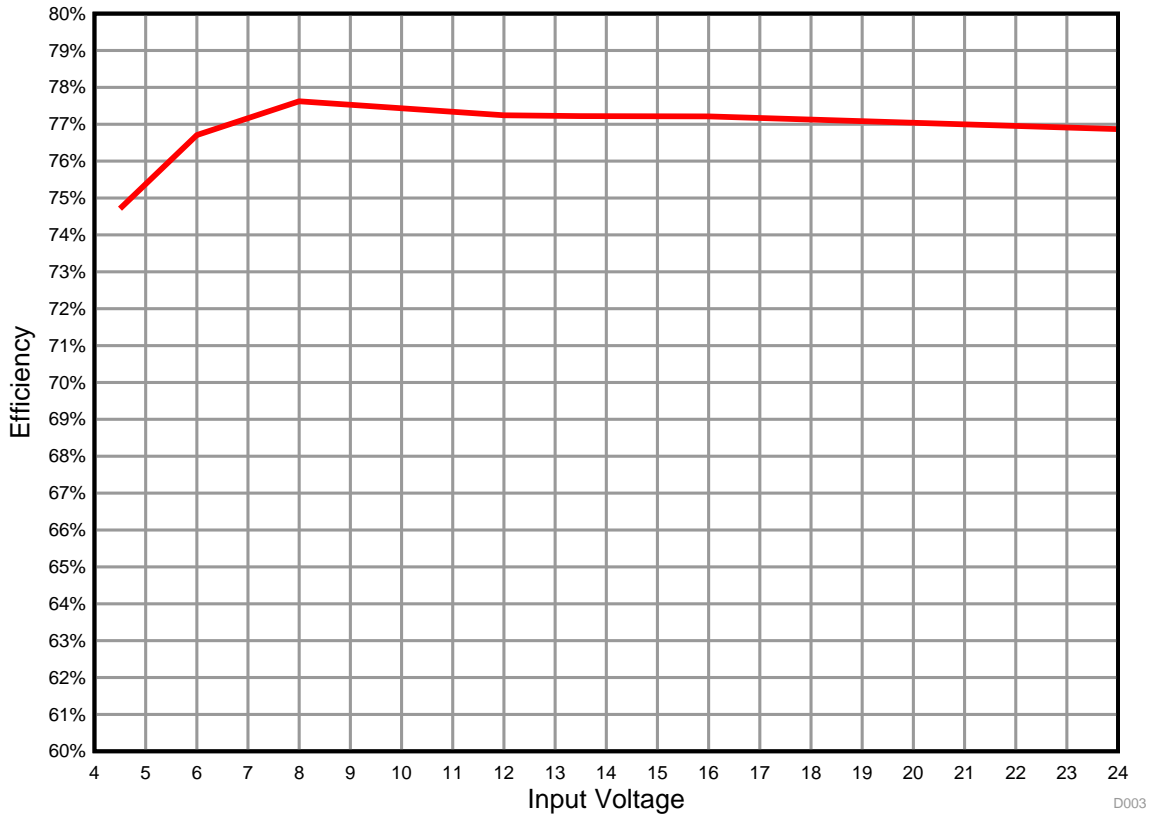


图 17. Two-Stage Efficiency

At the nominal input and full load, the two-stage efficiency is roughly 72%. The following  shows the total system efficiency with varying input voltage and the maximum specified loads for each supply.



D003_DD9.grf

图 18. Total System Efficiency for Varying Input Voltage

As expected, the measured peak efficiency appears to be around 8 V, with the efficiency decreasing only 0.5% as the input voltage increases from 8 V up to 24 V. At the nominal input voltage, the system efficiency is 77.22%. The following provides the system efficiency data used to generate the previous graph. The units for voltage, current, and power are V, A, and W, respectively.

表 2. System Efficiency Data

V _{IN} (V)	I _{IN} (A)	V _{OUT1} (V)	I _{OUT1} (A)	V _{OUT2} (V)	I _{OUT2} (A)	V _{OUT3} (V)	I _{OUT3} (A)	V _{OUT4} (V)	I _{OUT4} (A)	P _{IN} (W)	P _{OUT} (W)	EFFICIENCY (%)
4.5	4.527	0.873	10	1.198	2	1.798	2	4.98	0.100	20.3715	15.22	74.71
6	3.307	0.873	10	1.198	2	1.798	2	4.98	0.100	19.842	15.22	76.71
8	2.451	0.873	10	1.198	2	1.798	2	4.98	0.100	19.608	15.22	77.62
12	1.642	0.873	10	1.198	2	1.798	2	4.98	0.100	19.704	15.22	77.24
13.5	1.46	0.873	10	1.198	2	1.798	2	4.98	0.100	19.71	15.22	77.22
16	1.232	0.873	10	1.198	2	1.798	2	4.98	0.100	19.712	15.22	77.21
24	0.825	0.873	10	1.198	2	1.798	2	4.98	0.100	19.8	15.22	76.87

4.1.2 Switch Node Waveforms and Output Voltage Ripple

The following 图 19, 图 20, and 图 21 show the switch node and output voltage ripple at the full load of each DC-DC converter. The first set of scope shots shows the switch node for the main 3.3-V system supply, LMS3655-Q1, with a 4.5-V, 13.5-V, and 20-V input voltage. Channel 1 (yellow) shows the switch node waveform and channel 2 (pink) shows the output voltage ripple. The output voltage ripple measurements were AC coupled.

The scope shots show that the switching frequency of the supply sits around 416 kHz for all tested input conditions.

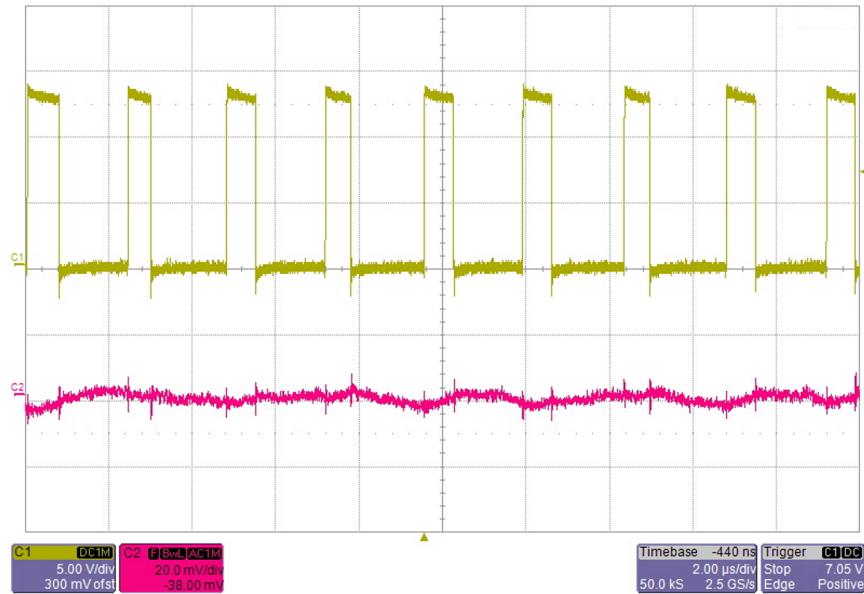


图 19. LMS3655-Q1 Switch Node and Output Voltage Ripple, 13.5-V Input at Full Load

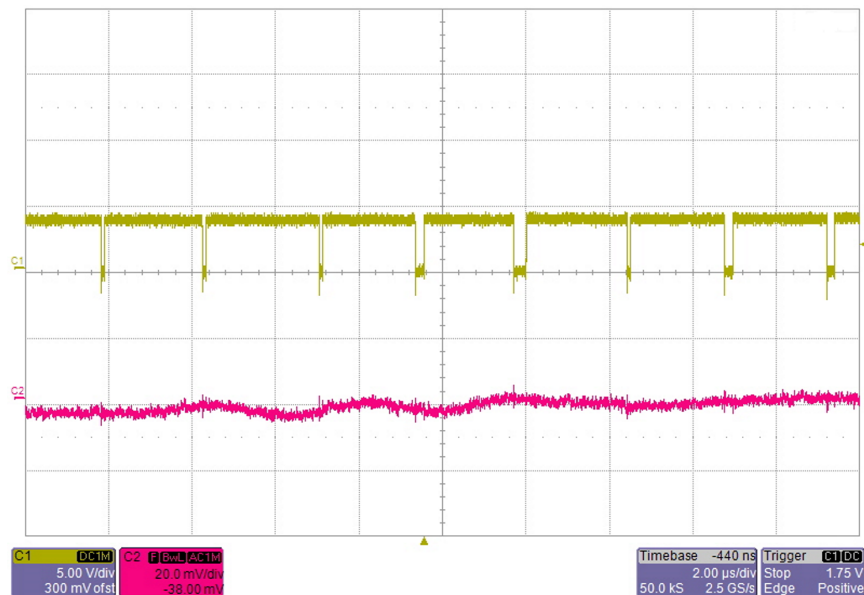


图 20. LMS3655-Q1 Switch Node and Output Voltage Ripple, 4.5-V Input at Full Load

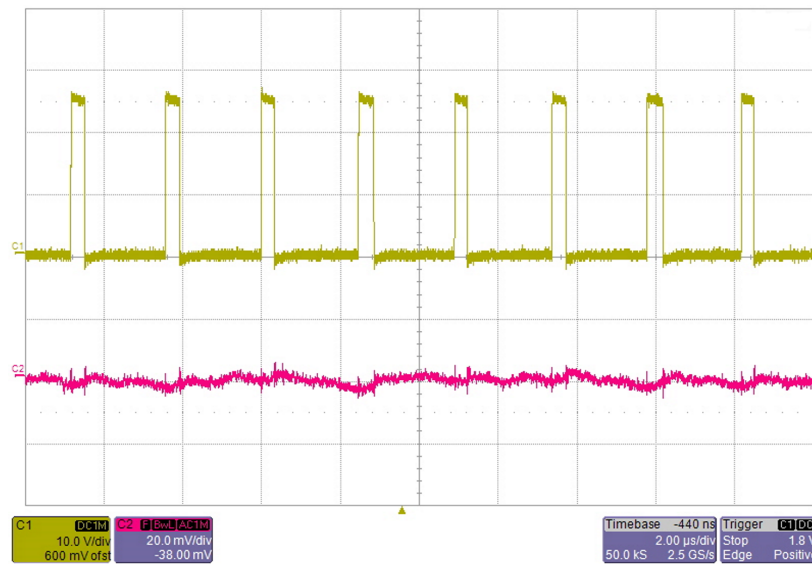


图 21. LMS3655-Q1 Switch Node and Output Voltage Ripple, 20-V Input at Full Load

图 22 和 图 23 显示内存和 I/O 电源的开关节点和输出电压纹波，LM26420-Q1。第一张示波器截图显示了 1.2-V 输出，随后是 1.8-V 输出。

这些截图显示开关频率为 2.29 MHz 左右，适用于两个开关器输出。

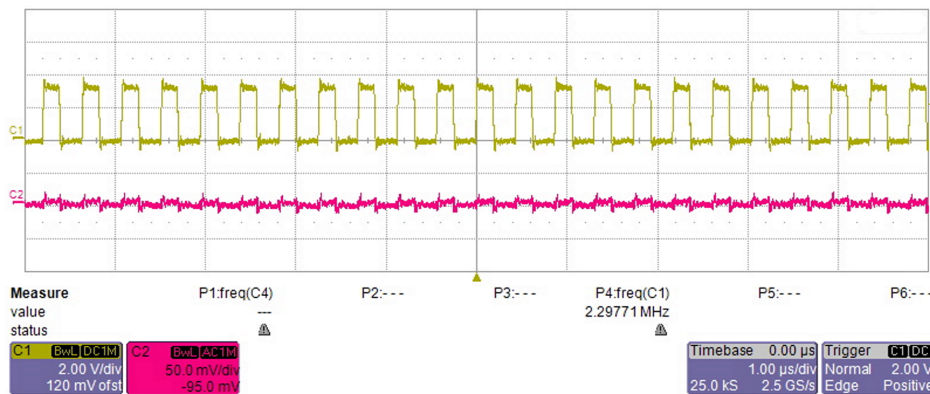


图 22. LM26420-Q1 Switch Node and Output Voltage Ripple, 1.2-V Output at Full Load

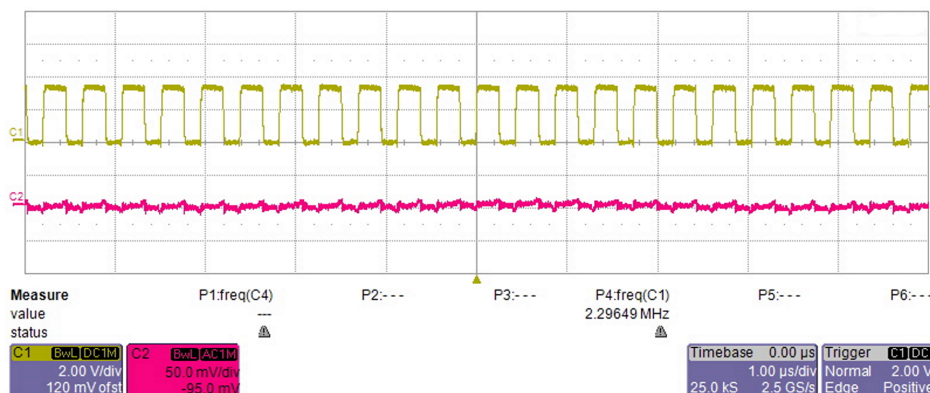


图 23. LM26420-Q1 Switch Node and Output Voltage Ripple, 1.8-V Output at Full Load

图 24 shows the 5-V CAN supply switch node and output voltage ripple. The switching frequency for the CAN supply is 2 MHz.

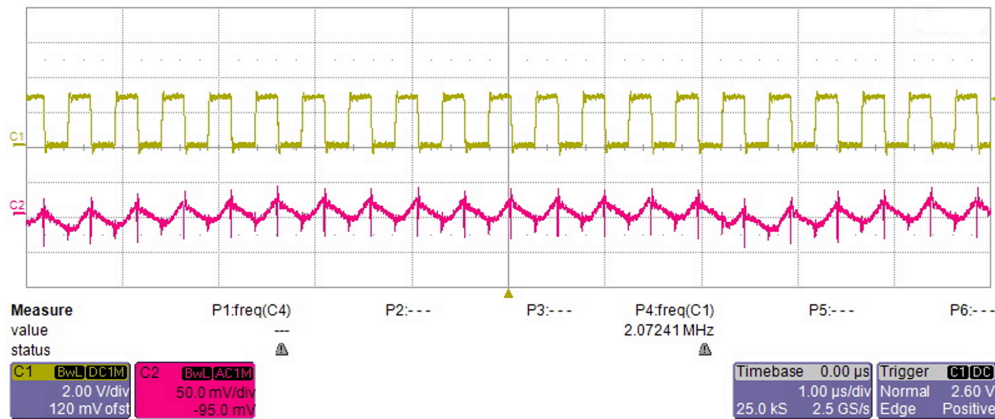


图 24. LM2775 Switch Node and Output Voltage Ripple, 5-V Output and Full Load

图 25 shows the switch node and output voltage ripple for the 0.9-V core-voltage supply. The switching frequency for the core-voltage supply is 1.9 MHz and the output voltage ripple is less than 5 mV.

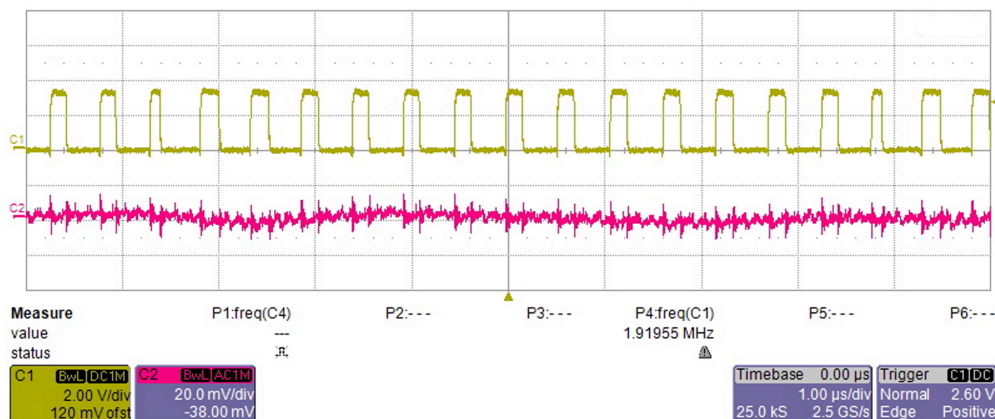


图 25. LP87561-Q1 Switch Node and Output Voltage Ripple, 0.9-V Output and Full Load

4.1.3 Load Transients

图 26 通过 图 29 展示了 50-100% 负载步变的瞬态响应，包括内存、I/O 电源、CAN 电源，以及核心电压电源的 50-100% 负载步变。通道 2 (粉色) 测量电流，通道 3 (蓝色) 进行 AC 耦合的输出电压纹波测量。

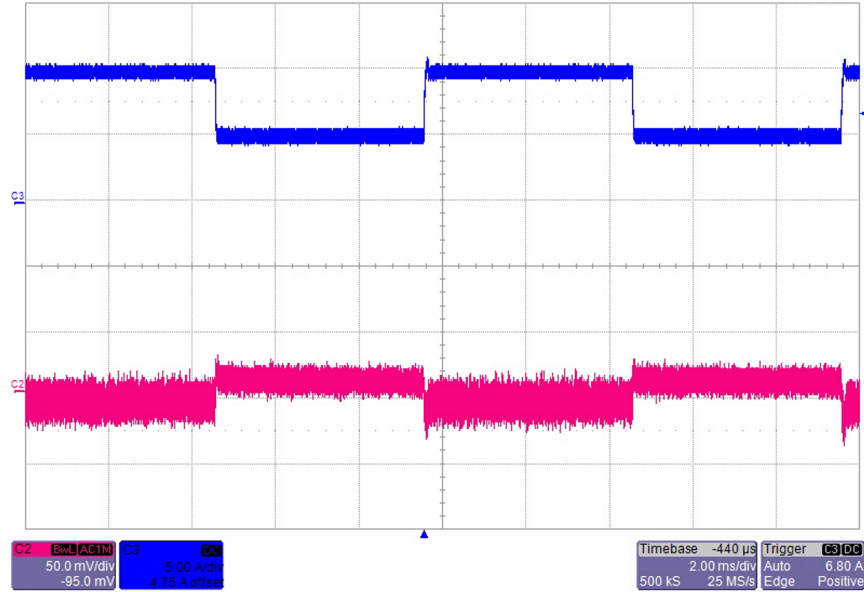


图 26. LP87561-Q1 50-100% Load Transient

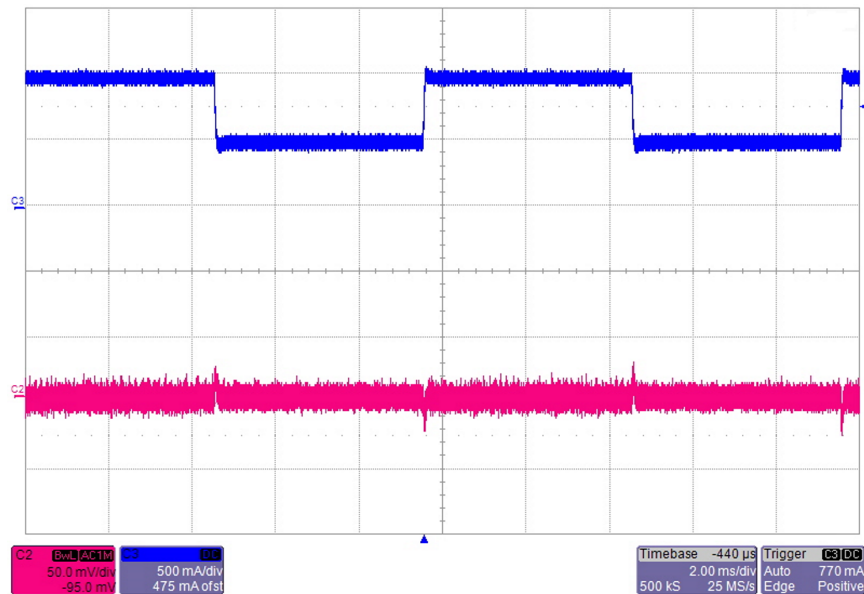


图 27. LM26420-Q1 50-100% Load Transient, 1.8 V

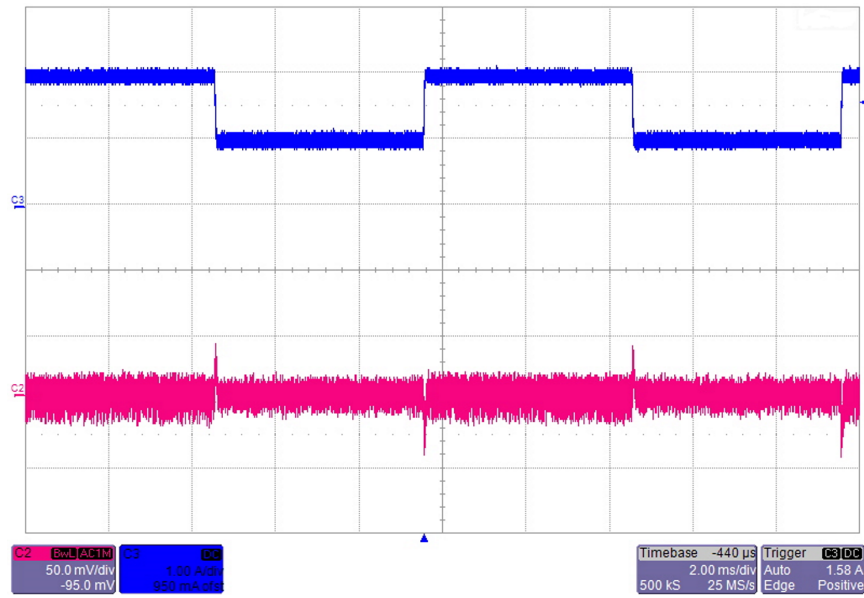


图 28. LM26420-Q1 50-100% Load Transient, 1.2 V

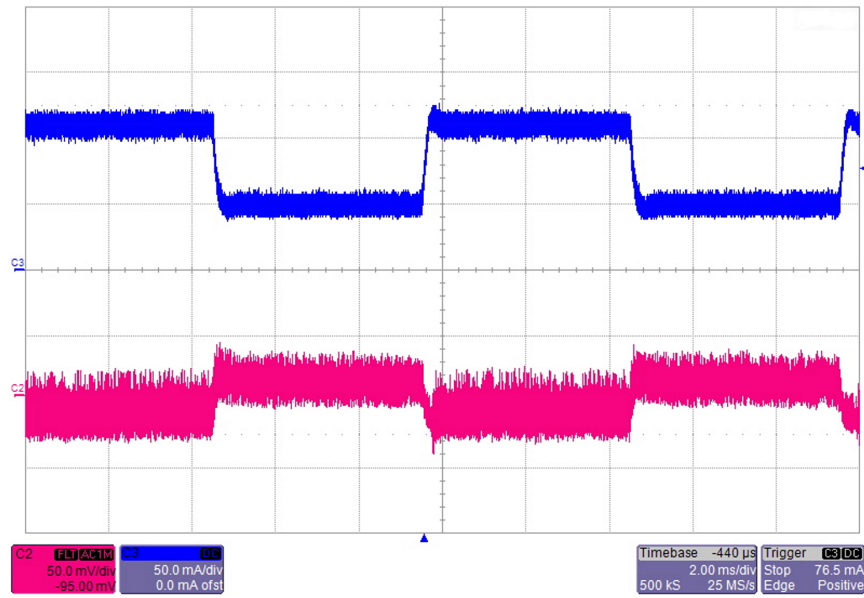


图 29. LM2775 50-100% Load Transient

4.1.4 Thermal Images

图 30 through 图 33 shows the temperature rise of each supply on the board under full load conditions and with a 13.5-V input voltage after 10 minutes.

注: Board temperatures can exceed 55°C during operation.

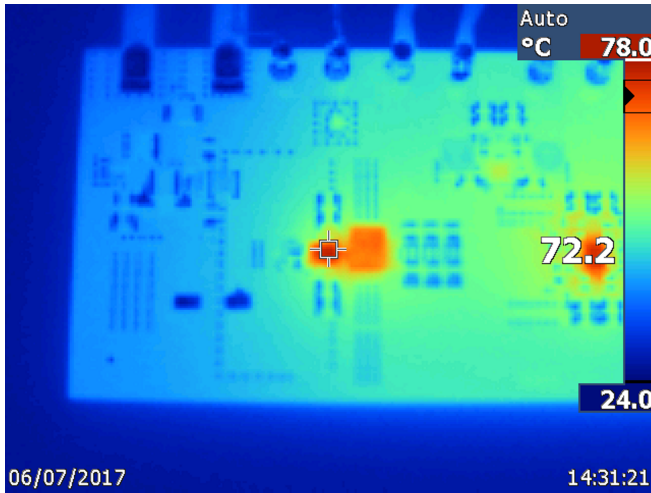


图 30. Thermal of LMS3655-Q1 at 5-A Load

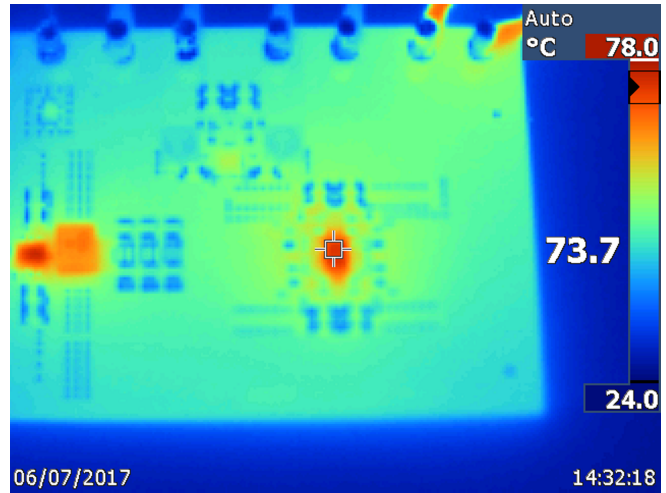


图 31. Thermal of LP87561-Q1 at 10-A Load



图 32. Thermal of LM26420-Q1 at 1 A for 1.8-V Rail and 2 A for 1.2-V Rail

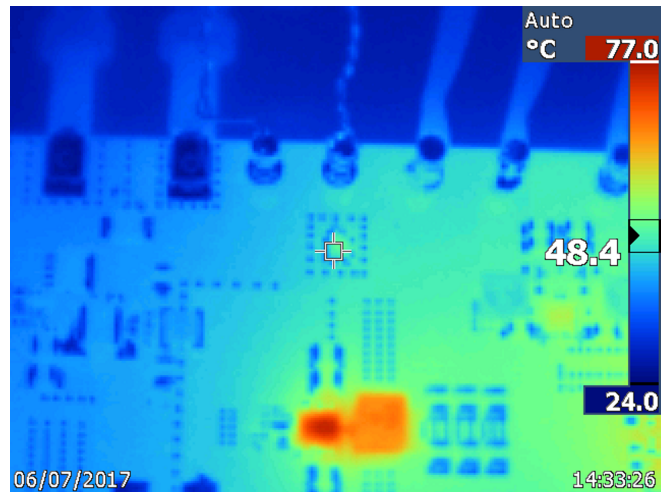


图 33. Thermal of LM2775 at 100-mA Load

4.1.5 Electrical Transient Testing

The following transients were tested:

- Reverse battery
- Cold crank
- Warm crank
- Start-stop

- Start-up and shutdown

The following subsections show the waveforms of each rail during each condition.

4.1.5.1 Reverse Battery

The following [图 34](#) shows that the input is disconnected during the reverse battery input voltage condition. Channel 4 is the input voltage and channel 1 is the input voltage after the LM74700-Q1 device.

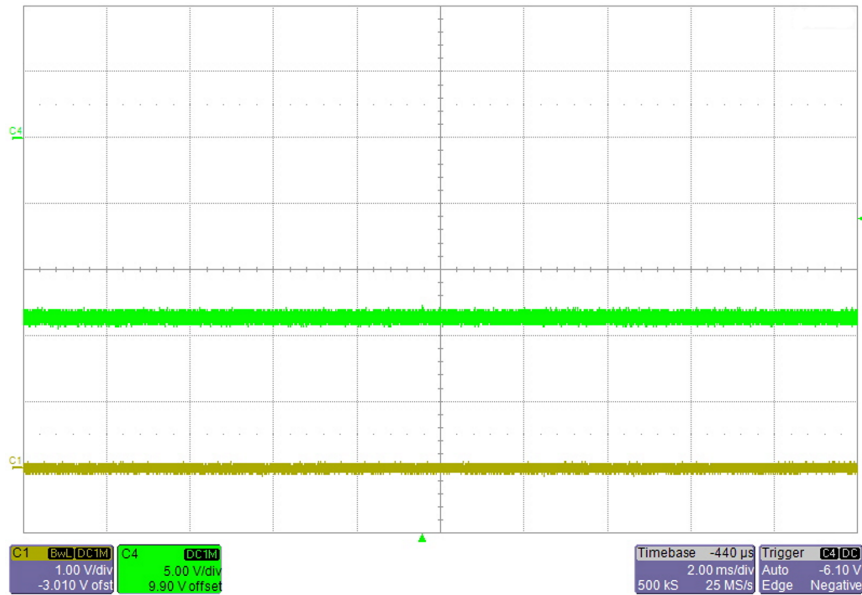


图 34. Continuous Reverse Voltage at Input

This behavior is expected from the LM74700-Q1 smart diode, where, upon a reverse voltage condition, the smart diode disconnects the system from the input. [图 35](#) shows the transition to reverse input voltage.

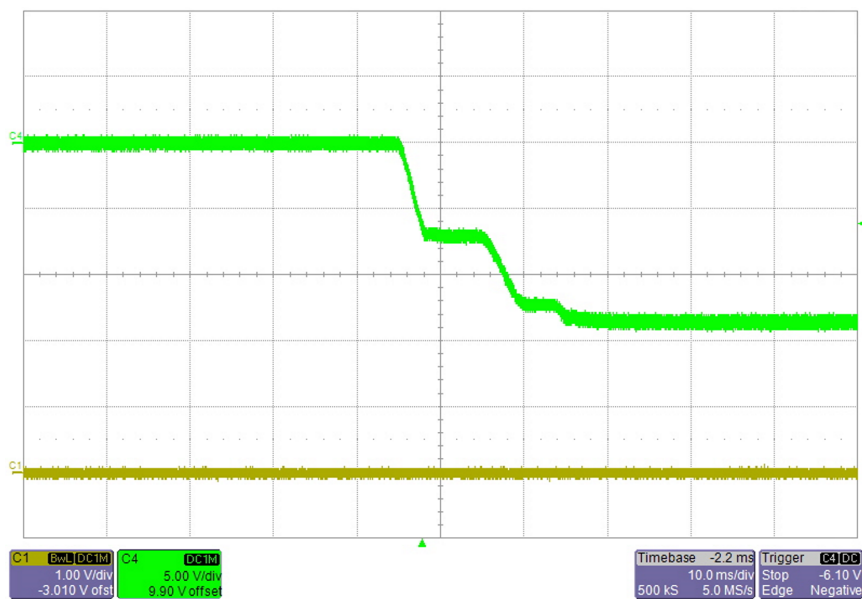


图 35. Transition to Reverse Voltage at Input

The input voltage after the smart diode remains undisturbed as the voltage at the input becomes increasingly negative.

4.1.5.2 Cold Crank

Testing this design for a severe cold-crank condition was a key objective. This test was accomplished without using a pre-boost.

For the cold-crank test, the input voltage was allowed to fall to 3.5 V from the nominal 13.5 V. 图 36 shows the cold-crank waveform.

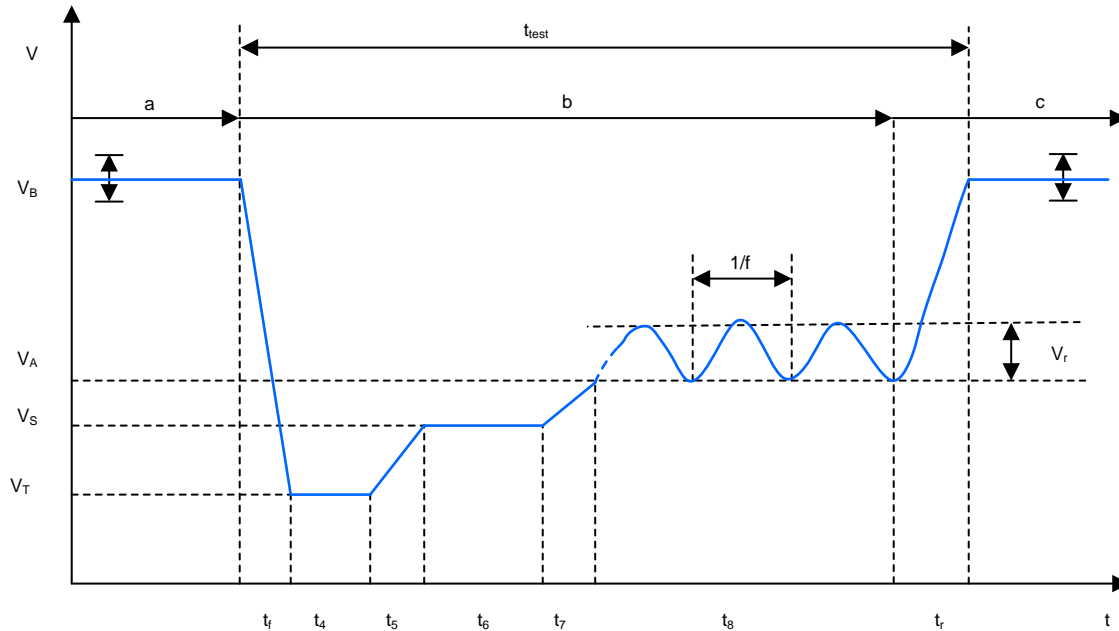
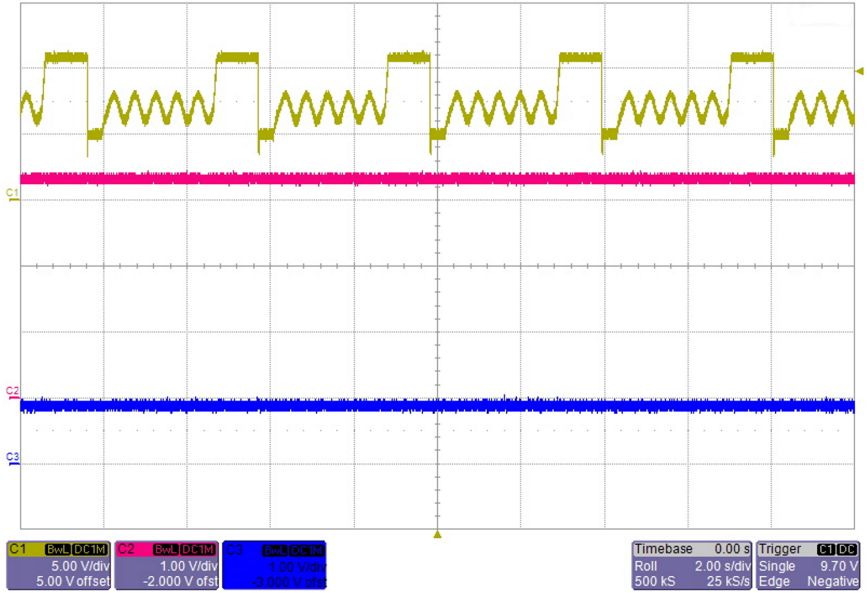


图 36. Cold-Crank Waveform and Parameters

表 3 list the cold-crank test pulse parameters.

表 3. Cold-Crank Test Pulse Parameters

PARAMETER	"NORMAL" TEST PULSE	"SEVERE" TEST PULSE
V_B	11.0 V	11.0 V
V_T	4.5 (0%, -4%)	3.2 V (0%, -4%)
V_S	4.5 (0%, -4%)	5.0 V (0%, -4%)
V_A	6.5 V (0%, -4%)	6.0 V (0%, -4%)
V_R	2 V	2 V
t_f	≤ 1 ms	≤ 1 ms
t_4	0 ms	19 ms
t_5	0 ms	≤ 1 ms
t_6	19 ms	329 ms
t_7	50 ms	50 ms
t_8	10 s	10 s
t_r	100 ms	100 ms
f	2 Hz	2 Hz

Only the severe test pulse was tested. The cold-crank condition lasts roughly 3.5 s, after which it repeats. In , channel 1 (yellow) shows the cold-crank input voltage waveform, channel 2 (pink) shows the 3.3-V output, and channel 3 (blue) shows the 0.9-V core-voltage supply output.

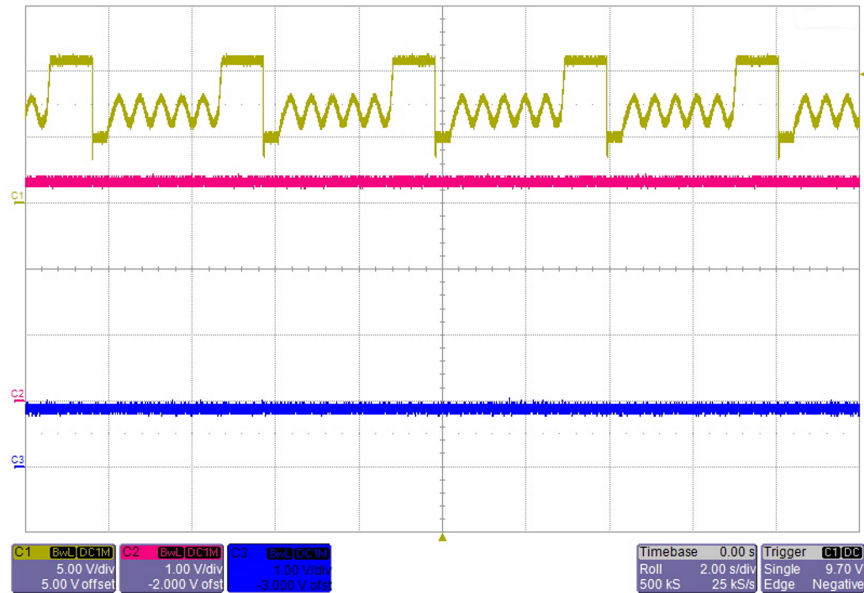
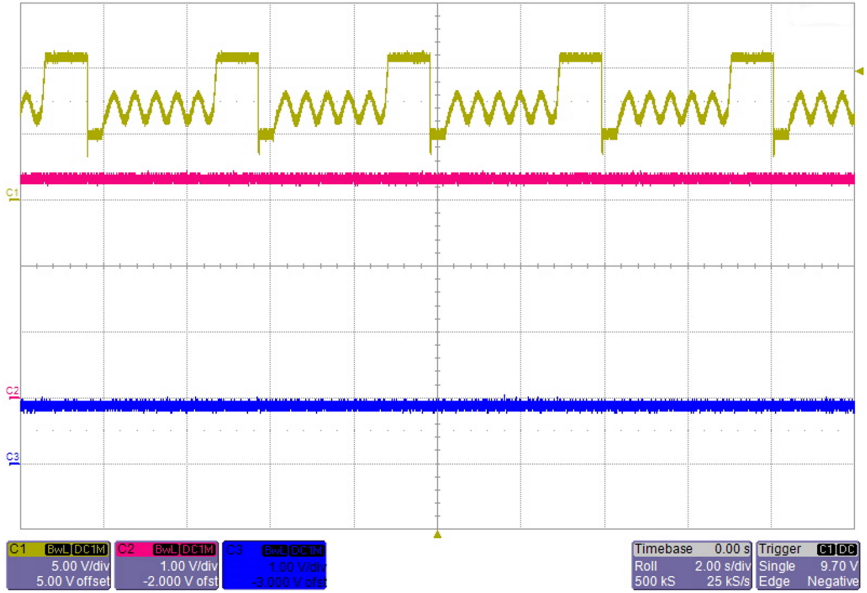
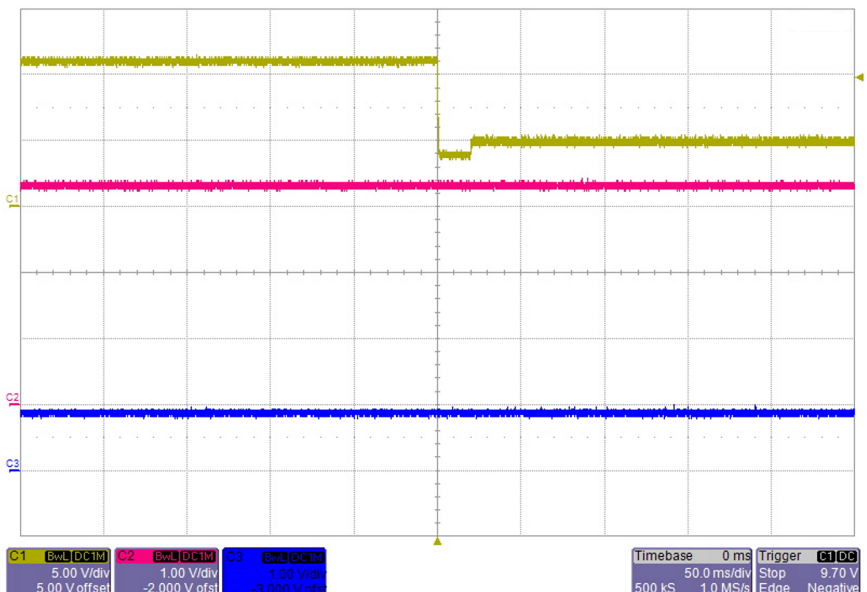


图 37. Cold Crank LP87561-Q1: 0.9 V at 10-A Output

Note that, in the previous , the output voltages are undisturbed by the cold-crank condition.  shows the initial drop from 13.5 V to 3.5 V in a shorter timescale.

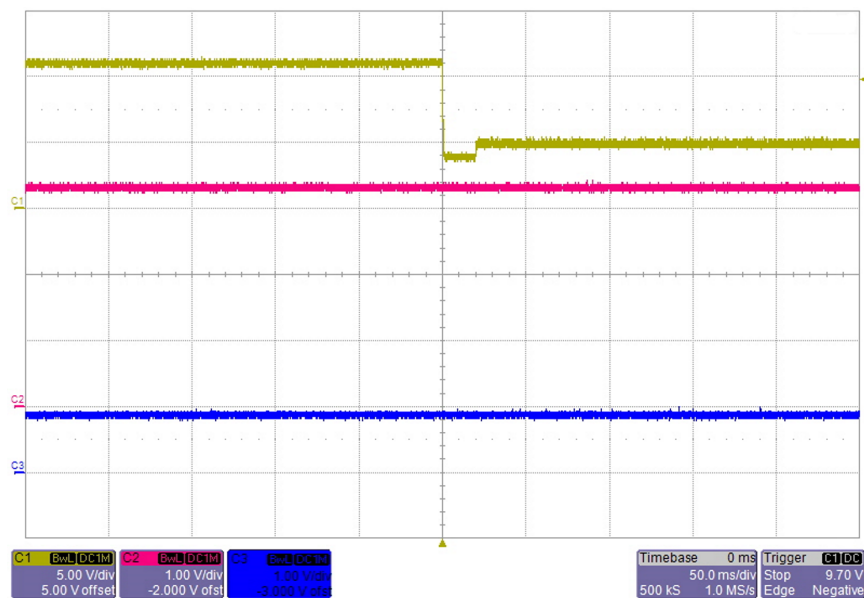


图 38. Cold Crank Down to 3.5 V, LP87561-Q1: 0.9 V at 10-A Output

The initial drop on a shorter timescale still shows no disturbance to the output of the supplies.

4.1.5.3 Warm Crank

This subsection provides test data for the main system supply and core-voltage rails during warm-crank conditions. In [图 39](#) and [图 40](#), channel 1 (yellow) measures the warm-crank input voltage waveform, channel 2 (pink) measures the 3.3-V main system supply, and channel 3 (blue) measures the 0.9-V core-voltage supply.

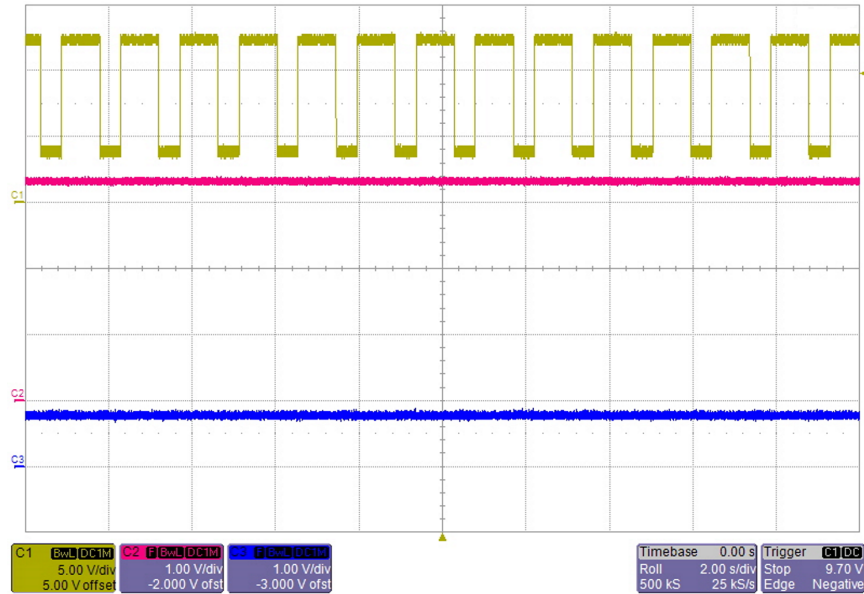


图 39. Warm Crank LP87561-Q1: 0.9 V at 10-A Output

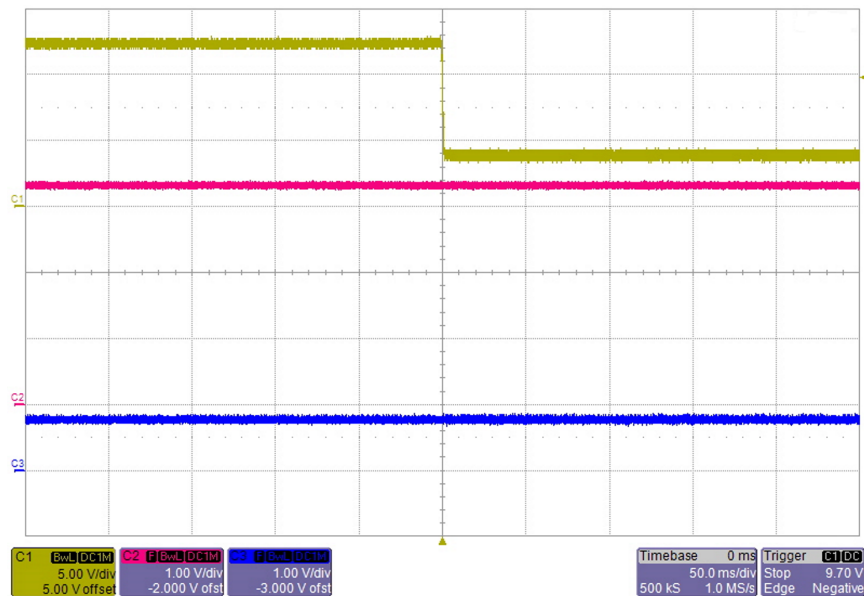


图 40. Warm Crank 50-ms Timescale

Both figures show the output of the supplies to be undisturbed during the warm-crank condition.

4.1.5.4 Start-Stop

This subsection provides test data for the main system supply and core-voltage rails during start-stop conditions. In [图 41](#) and [图 42](#), channel 1 (yellow) measures the start-stop input voltage waveform, channel 2 (pink) measures the 3.3-V main system supply, and channel 3 (blue) measures the 0.9-V core-voltage supply.

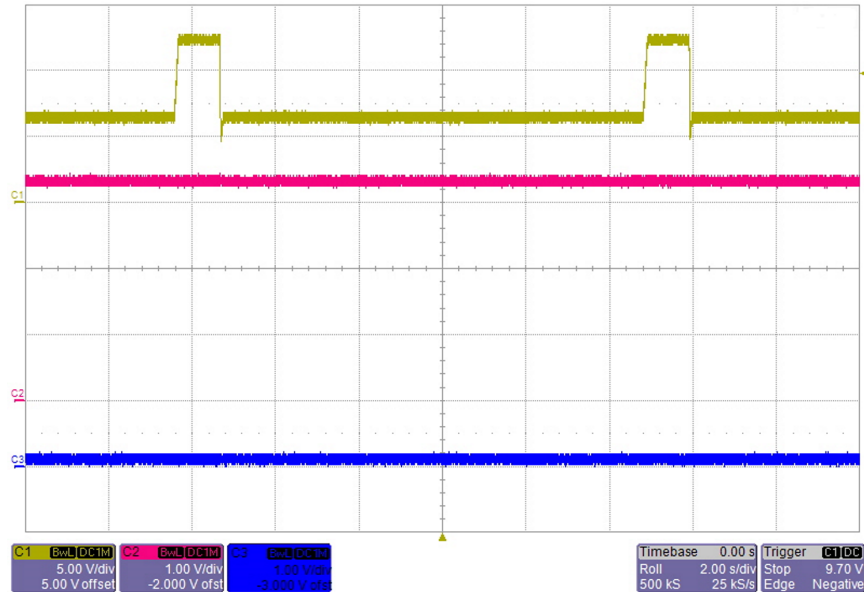


图 41. Start-Stop 5-s Timescale, 0.9 V at 10-A Output

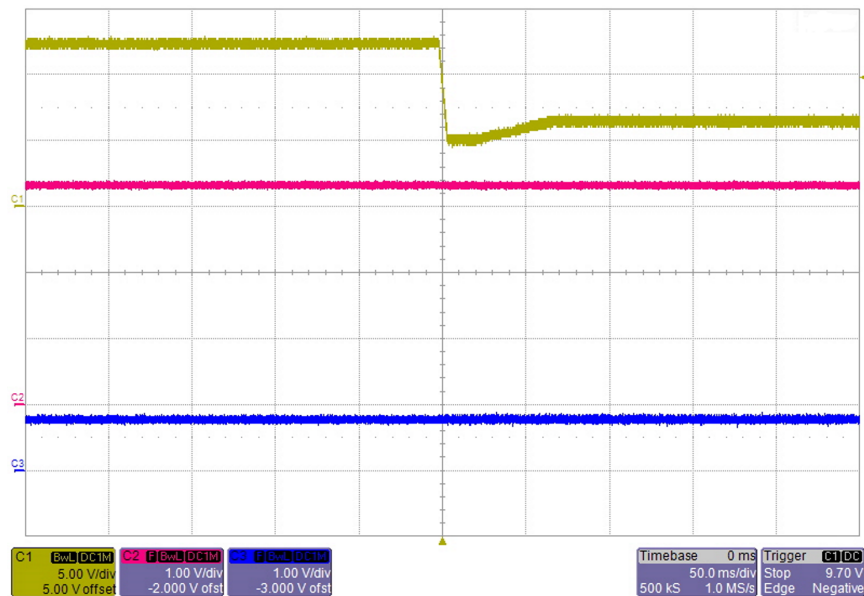
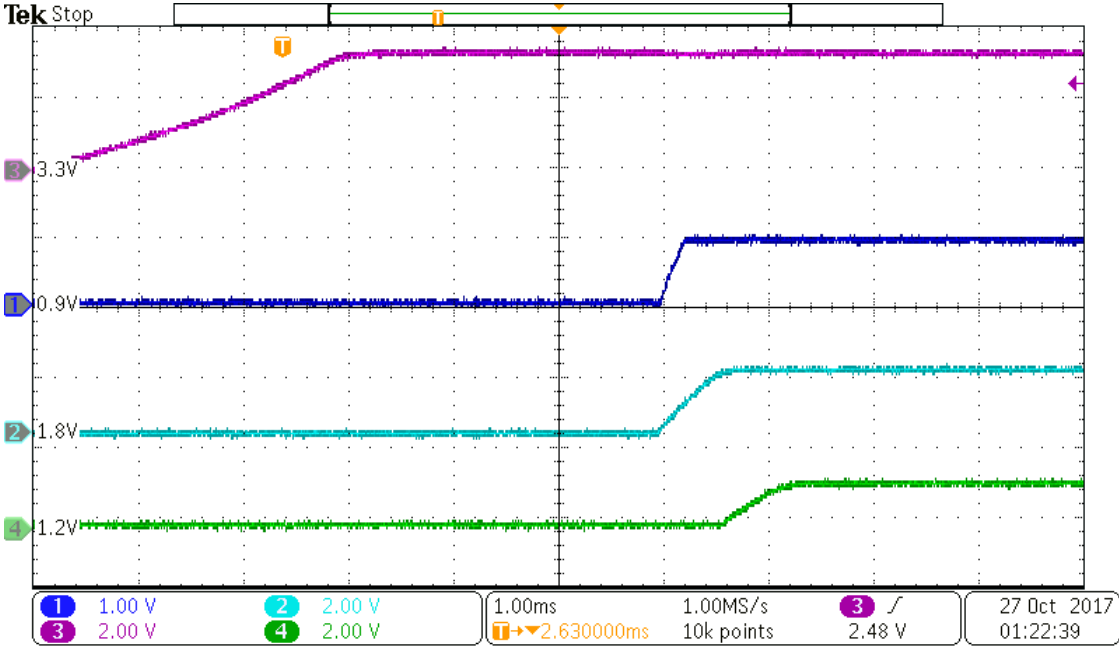
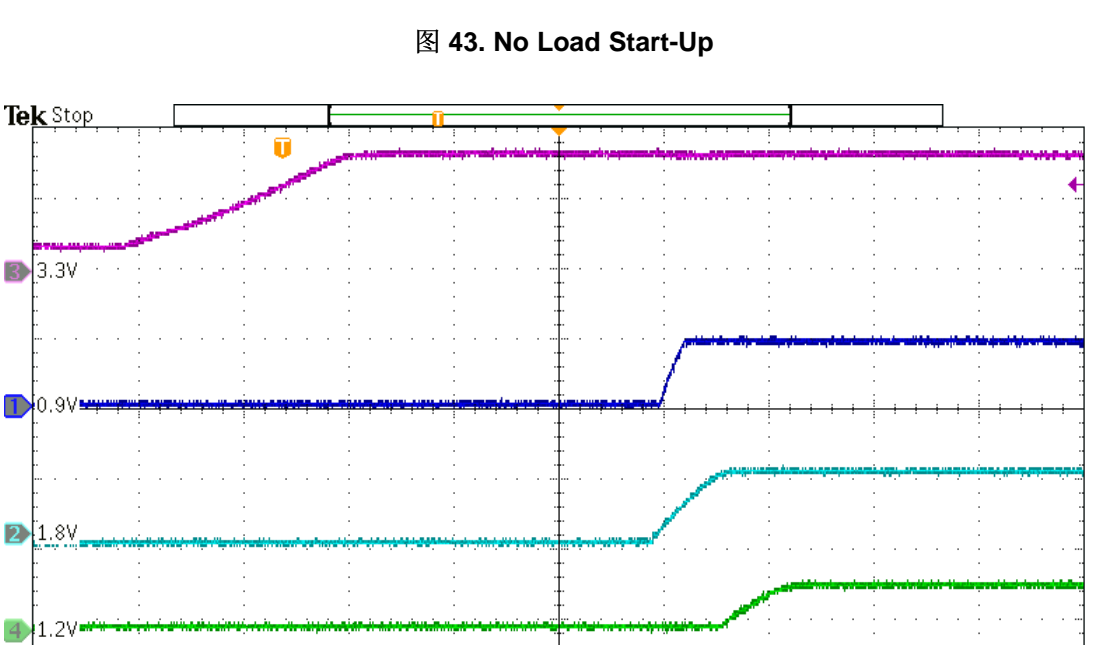


图 42. Start-Stop 50-ms Timescale, 0.9 V at 10-A Output

Both figures show the output of the supplies to be undisturbed during the start-stop condition.

4.1.5.5 Start-Up and Shutdown

This subsection provides test data for the core-voltage, CAN, and I/O supplies during system start-up and shutdown. Measurements were taken at full and no loads for each supply. In the following  through , channel 1 (yellow) measures the input voltage waveform, channel 2 (pink) measures the 0.9-V core-voltage supply, channel 3 (blue) measures the 1.8-V I/O supply, and channel 4 (green) measures the 5-V CAN supply.

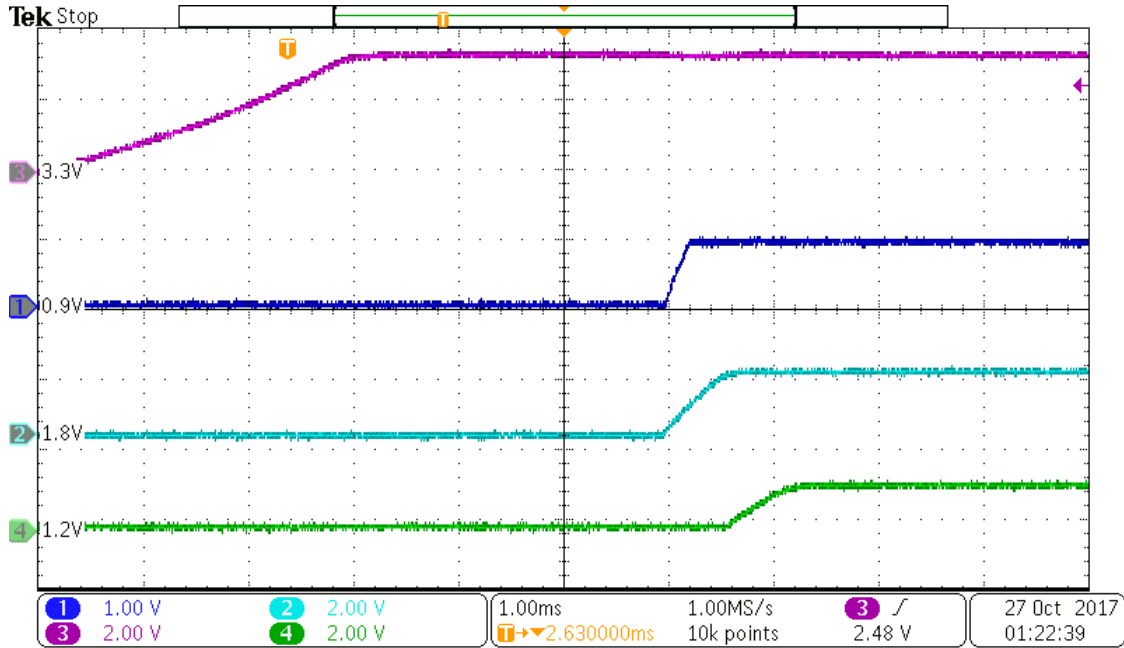


图 43. No Load Start-Up

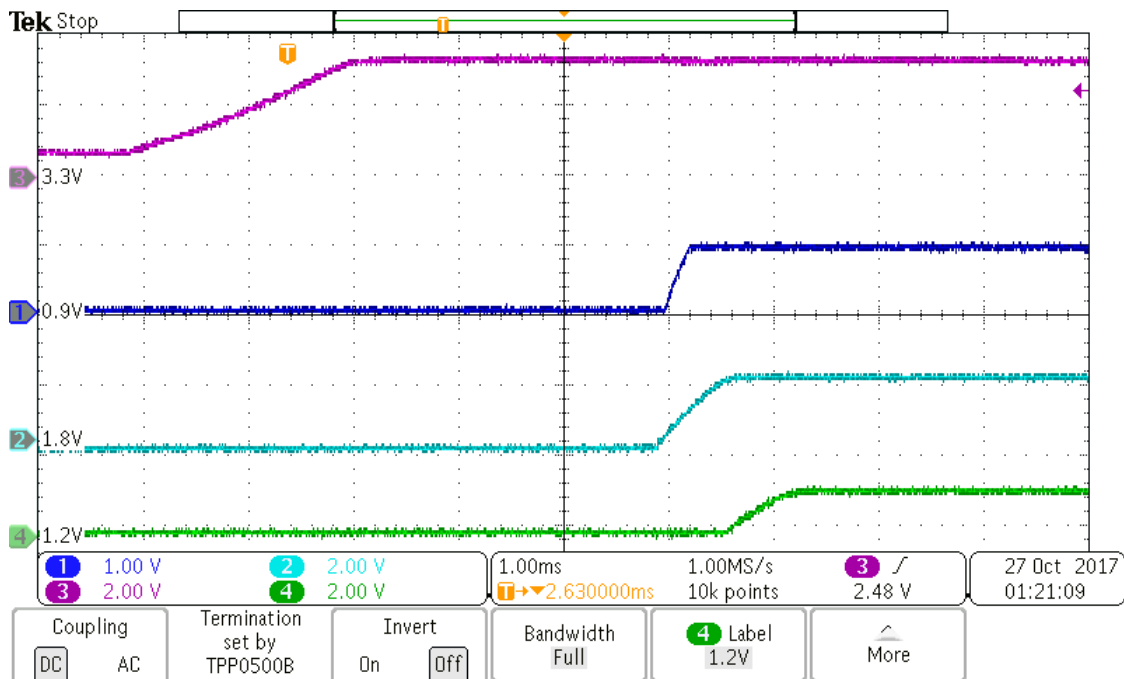


图 44. Full Load Start-Up

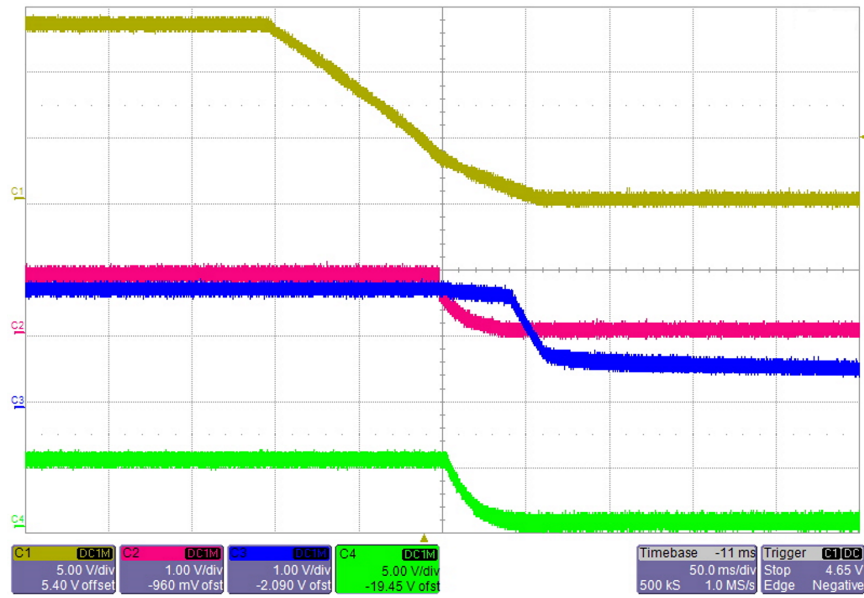


图 45. No Load Shutdown

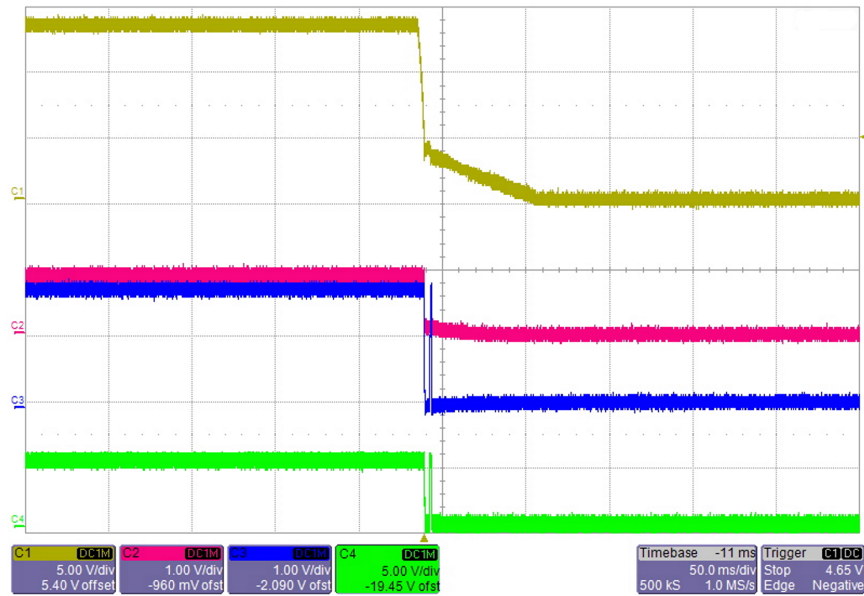


图 46. Full Load Shutdown

4.1.6 Conducted Emissions

The conducted emissions of the TIDA-01524 have been tested against CISPR 25 Class 5 limit lines. The examined frequency band spans from 150 kHz to 108 MHz covering the AM-FM radio bands, very-high-frequency (VHF) band, and TV band specified in CISPR 25.

图 47 和 图 48 显示测试结果。图 47 显示测试结果使用峰值检测器和平均检测器测量，分别，高达 30 MHz。图 48 显示测试结果使用平均检测器和峰值检测器测量从 30 MHz 到 108 MHz。限制线（显示为红色）是 CISPR 25 中规定的 Class 5 传导干扰限值。黄色迹线（峰值检测器测量）和蓝色迹线（平均检测器测量）是测量结果。

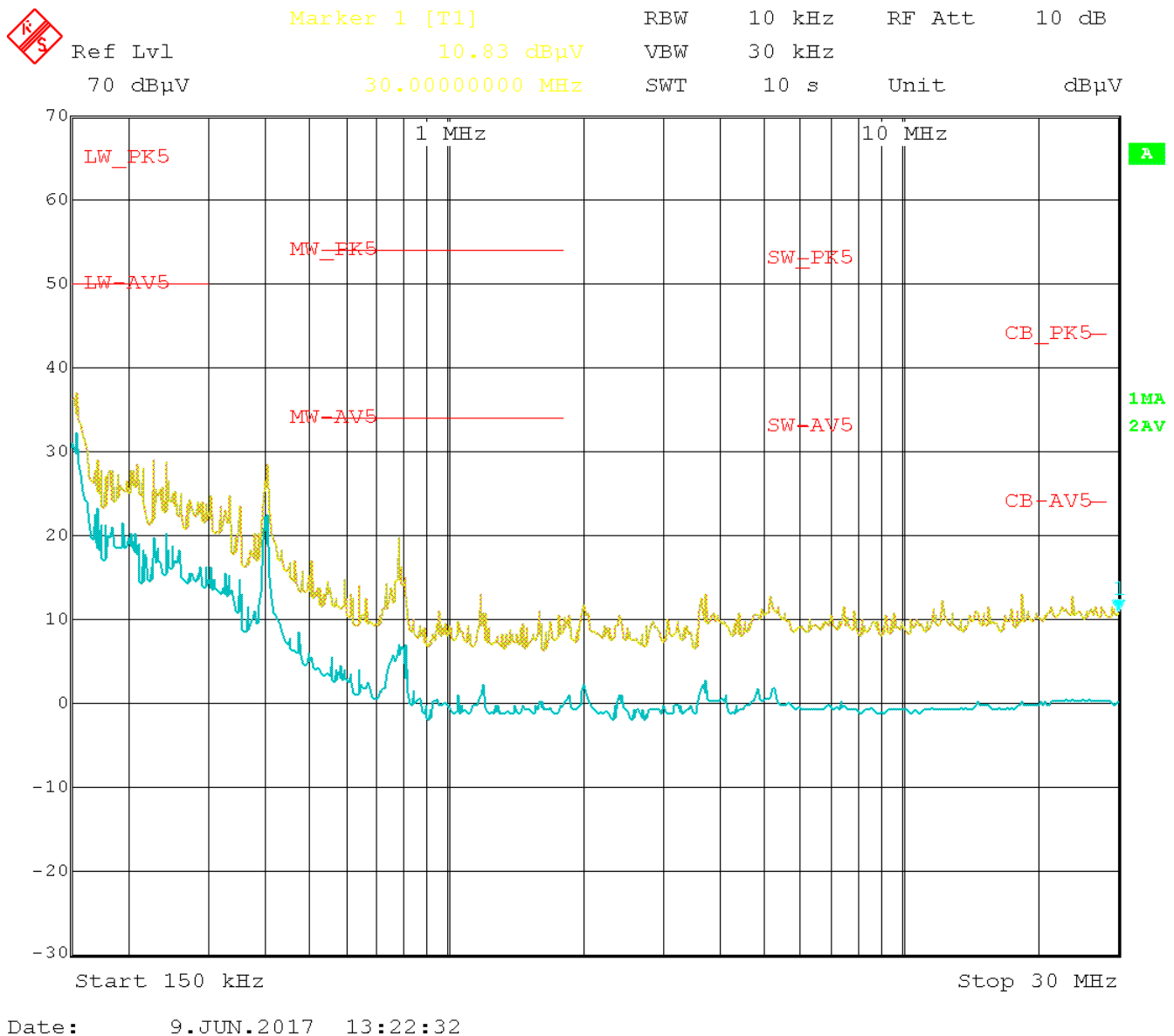
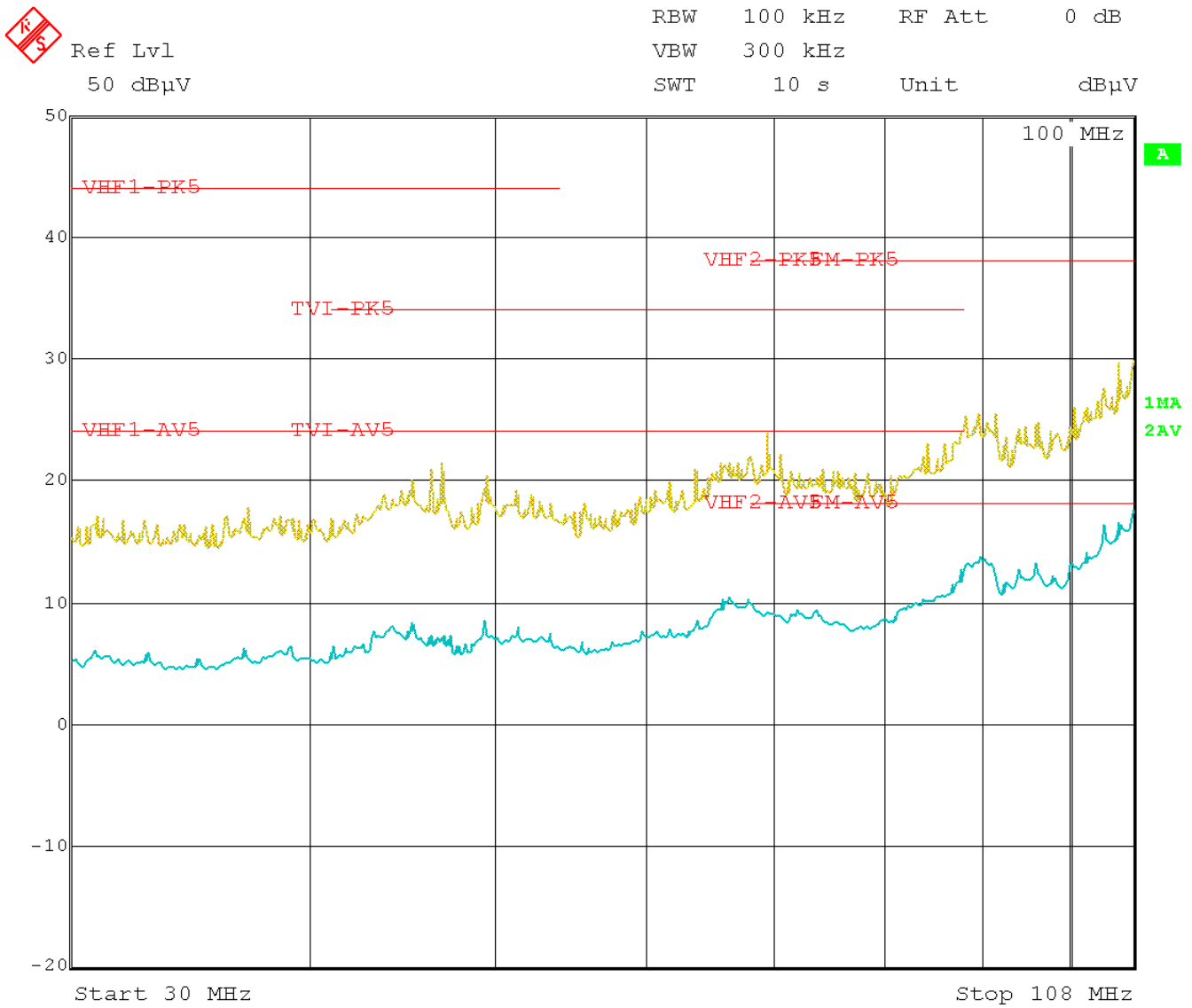


图 47. 150-kHz to 30-MHz Conducted Emissions—Peak and Average Detection



Date: 9.JUN.2017 13:21:43

图 48. 30-MHz to 108-MHz Conducted Emissions—Peak and Average Detection

5 Design Files

To download the design files for this TI Design including the schematic, bill of materials, layer plots, Gerber files, and Altium files, see the design files at [TIDA-01524](#).

5.1 PCB Layout Recommendations

5.1.1 Input Protection Circuitry

Place input protection circuitry as close to the battery terminal inputs as possible, rather than close to the downstream circuit it is protecting, to reduce the inductance of the path. This placement allows the TVS diodes to react as quick as possible to any transients. Close placement provides a tight loop for the return path back to the battery terminals while the TVS diodes shunt a transient event. In the event of a reverse polarity event, the FET Q1 quickly shuts off, possibly causing inductive kicks due to the interrupted current flow. The severity of this kick is a function of the inductance and, therefore, the length and width of the power path.

5.1.2 Input EMI Filter Considerations

The goal of the EMI filter is to minimize emissions, especially conducted emissions. The key to minimizing emissions is providing low impedance paths to quickly ground high-frequency noise, which is typically accomplished by containing high-frequency current loops. 图 49 shows the current flow through the EMI filter. The DC is outlined in red and the high-frequency AC paths are outlined in green.

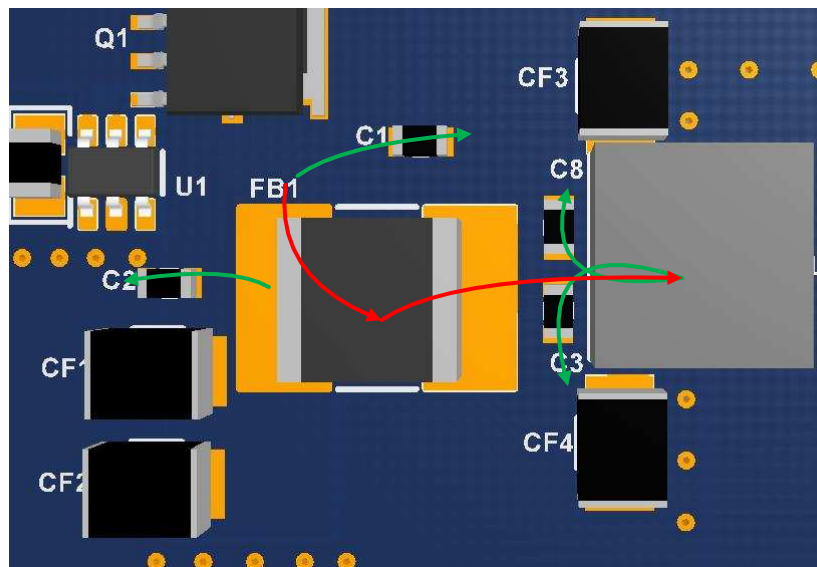


图 49. Input EMI Filter

Conducted emissions are mainly due to high-frequency noise that input capacitors cannot bypass. This noise is conducted onto the input leads of the supply, which drives the convention that the higher-frequency AC flows away from the 3.3-V supply back toward the system supply.

图 49 shows the smaller 0.1- μ F capacitors C3 and C8 close to the 4.7- μ H inductor LF1 to filter out the high-frequency noise not attenuated by the inductor. Capacitors C3 and C8 are placed across from each other instead of next to each other to minimize the possibility for inductive coupling during operation due to their close proximity.

Inductors behave capacitively above their resonant frequency; therefore, any frequencies above this are not attenuated. The amount of noise that is conducted back onto the supply line directly depends on how much has been filtered out; therefore, the shortest path to ground for high-frequency noise is required.

5.1.3 Noise-Sensitive Traces and Components

The feedback (FB) and compensation (COMP) nodes of power supplies are especially high impedance and thus susceptible to picking up noise. These nodes are critical to operate the control loop of the device; therefore, poor placement and routing of these components or traces can affect the performance of the device and system by introducing unwanted parasitic inductances and capacitances.

The switch node of DC-DC converters are typically very noisy. The switch node can radiate a significant amount of energy and can couple noise into sensitive lines. Traces for the switch node must be wide enough for the maximum current but small enough to minimize radiation. Signals like output voltage FB traces for power supplies are high-impedance lines. These signals are quite sensitive to disturbances, especially to noise from switch nodes and high-bandwidth I²C lines. Placing sensitive traces apart from noisy traces, ideally on the opposite sides of the board or separate layers (with ground planes between them), mitigates such negative effects. The FB loop itself, from output voltage to FB pin and analog ground, must be small enough to minimize parasitics and noise susceptibility. Place all analog and control loop components such that their trace lengths back to the IC are minimized.

图 50 shows the component placement of the main 3.3-V supply on the TIDA-01524 PCB. High frequency filter capacitors are placed closest to the input of U2 to minimize the loop area of high di/dt currents. As discussed in 图 50, the LMS3655-Q1 comes in the HotRod package which reduces pin inductance and magnetic field from currents. This reduction in magnetic field comes from having the input pins on opposite sides of the device. Note in the following figure 图 50 Cin_hf1 and Cin_hf2 both as close to the device as possible and are on opposing sides, and that the feedback network is on the top left of the image, away from the switch node and high di/dt current loops.

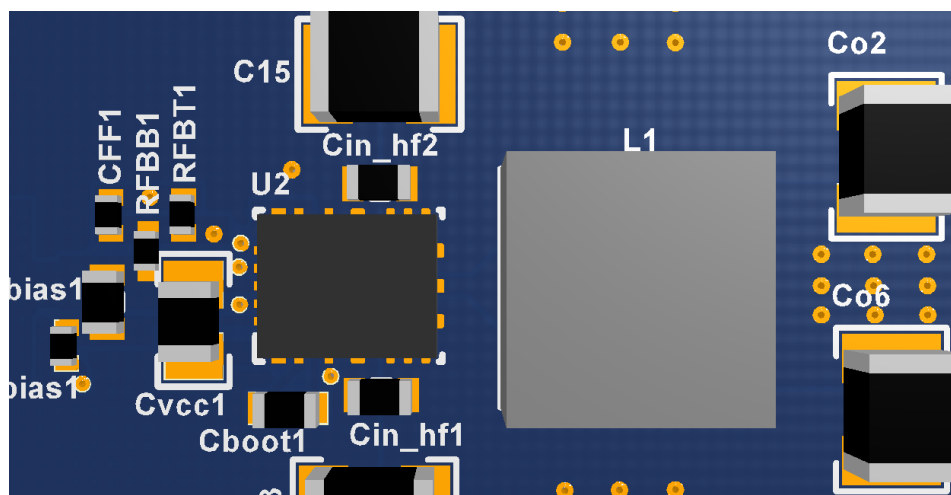


图 50. 3.3-V Supply Component Placement

The 3.3-V output connects to a power plane on middle layer 3 through the vias shown near Co6. This 3.3-V power plane connects to the rest of the system supplies, and extends close to the feedback network, where the output voltage is sensed.

Similar layout considerations have been made for the 0.9-V core-voltage supply. 图 51 shows the FB trace of the core-voltage supply output routed on layer 3, which is several millimeters away from the switch node.

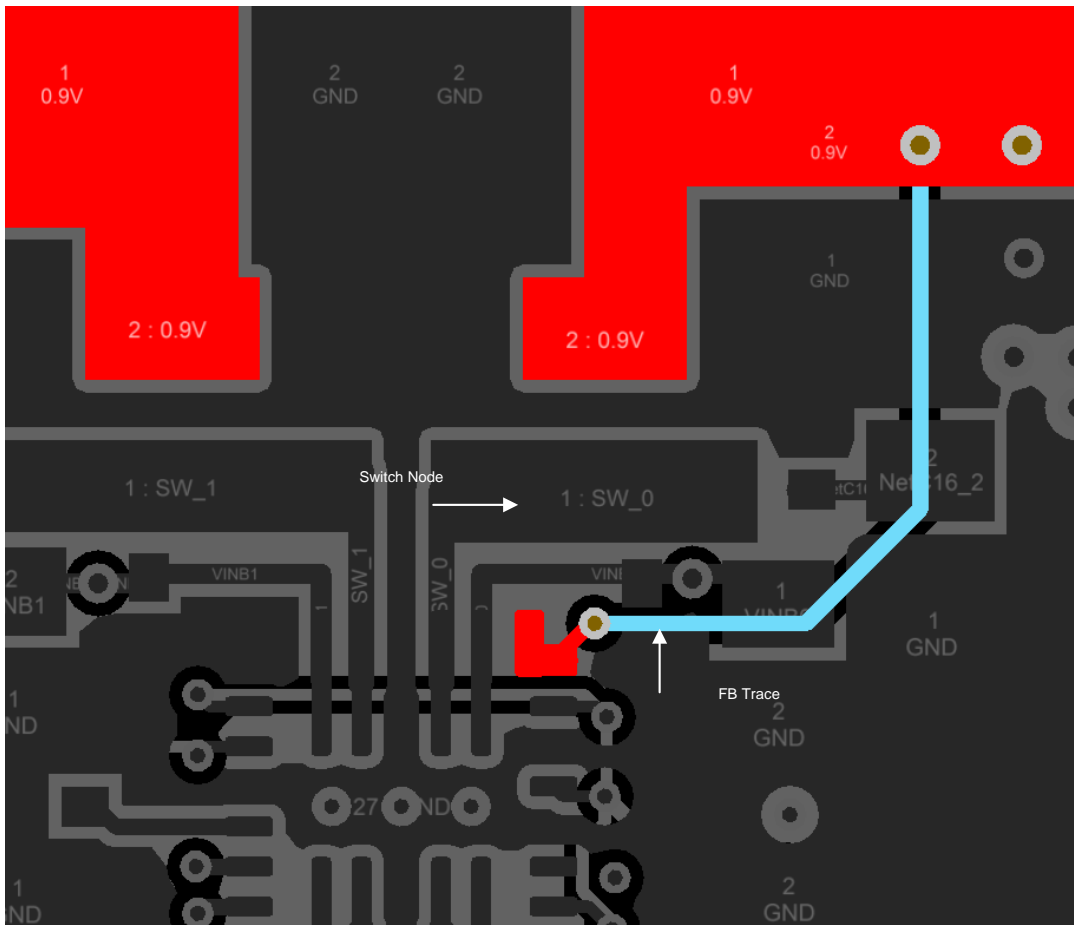


图 51. Routing Feedback Traces Around Switch Nodes

5.1.4 EMI Mitigation for Core-Voltage Supply

This subsection covers the layout for the filtering circuitry for the 0.9-V core-voltage supply. Because this supply provides the most current, more considerations have been made to mitigate EMI, which includes both the snubber circuits and input EMI filters for each phase. For more theory on EMI reduction for DC-DC converters, see [AN-2155 Layout Tips for EMI Reduction in DC / DC Converters](#) (SNVA638). The following [图 52](#) and [图 53](#) show the external component placement for the 0.9-V core-voltage supply.

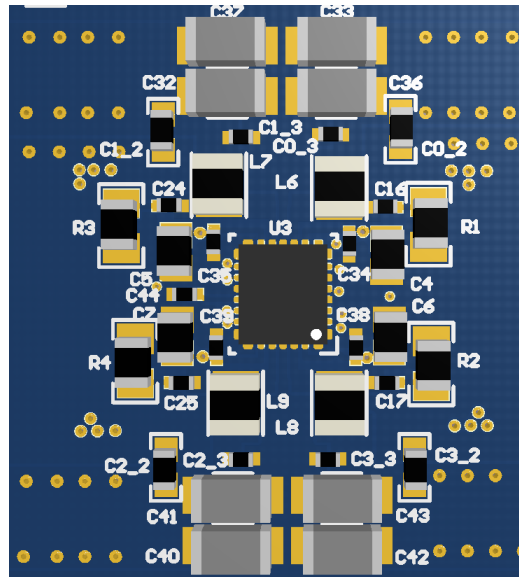


图 52. Core-Voltage Supply Component Placement—Top View

Note that, on the top layer, the 0.9-V output voltage plane encircles the entire solution and each buck has its own quadrant with high-frequency filter circuitry in close proximity with the IC.

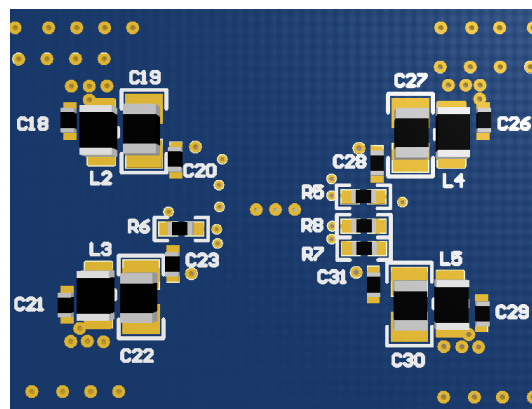


图 53. Core-Voltage Supply Passives Placement—Bottom View

The same rule for high-frequency filtering has been followed on the bottom layer. The main goal is to ensure that high-frequency current loops are as small as possible. High-frequency decoupling caps are located on both sides of the board by the device input to minimize the current loop area by providing a low impedance path for high-frequency input currents. For example, observe in [图 53](#) that buck 0 uses C20 (top-center left) and C34 (top-center right of [图 52](#)) for high-frequency decoupling.

The layout screen shot shown in 图 54 focuses on the components for buck 0 and the arrows to show current flow. The dashed arrows represent switching current. The green dashed arrow shows the switching current flow through the snubber circuit (C16 to R1) to ground.

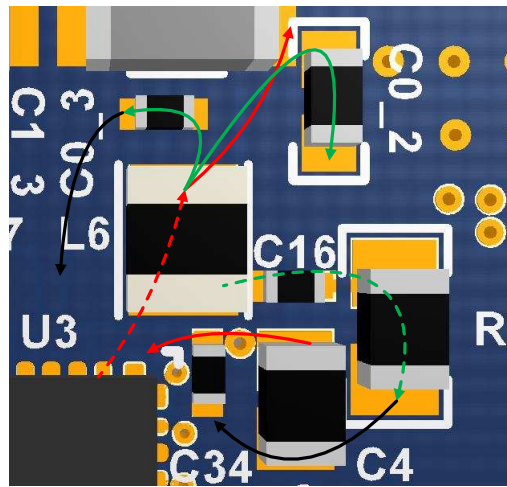
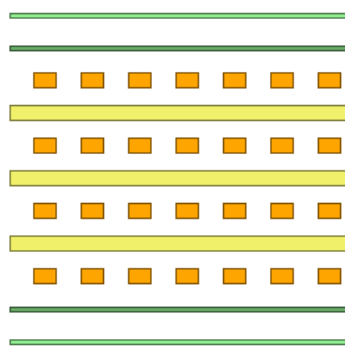


图 54. AC and DC Flow Through Snubber Circuit and Output Filter

Note that the snubber circuit is closest to the input of buck 0 instead of the output. This placement is intended to minimize the current loop of the high-frequency currents that flow from the input capacitors, to the switch node, and back to the input capacitors. For example, if the snubber is placed above inductor L6 near C0_3, the high-frequency current loop is much larger to return to input capacitors C34 and C4. This larger current loop can interfere with other nearby circuits and current loops and introduce other EMI problems.

5.1.5 PCB Layering Recommendations

If using a six-layer board, make layers 2 and 5 ground planes to shield the internal signal layers from outside noise sources as well as the switch nodes found on the top layer. If using a four-layer board (as in this reference design), layer 2 must be a ground plane. 图 45 details the stack-up used in this reference design.



Layer Name	Type	Material	Thickness (mil)	Dielectric Material	Dielectric Constant
Top Overlay	Overlay				
Top Solder	Solder Mask/Co...	Surface Material	0.4	Solder Resist	3.5
Top Layer	Signal	Copper	2.8		
Dielectric 2	Dielectric	Core	10	FR-4	4.2
Signal Layer 1	Signal	Copper	1.4		
Dielectric 3	Dielectric	Core	10	FR-4	4.2
Signal Layer 2	Signal	Copper	1.4		
Dielectric1	Dielectric	Core	10	FR-4	4.2
Bottom Layer	Signal	Copper	2.8		
Bottom Solder	Solder Mask/Co...	Surface Material	0.4	Solder Resist	3.5
Bottom Overlay	Overlay				

图 55. Layer Stack-Up With GND Planes Separating Signal Layers

Keep power traces and pours on the same layer as much as routing requirements allow. This grouping minimizes the inductance of the path and reduces noise coupling between planes. Unfortunately, due to the high number of rails in this reference design and the routing requirements required to get signals to the EVM connectors, sticking to this rule is not totally possible.

6 Related Documentation

1. Texas Instruments, [5.5-A, 36-V, Synchronous, 400-kHz Step-Down Converter](#)
2. Texas Instruments, [Four-Phase 16-A Buck Converter With Integrated Switches](#)
3. Texas Instruments, [Dual 2-A Automotive-Qualified, High-Efficiency Synchronous DC-DC Converter](#)
4. Texas Instruments, [Switched Capacitor 5-V Boost Converter](#)
5. Texas Instruments, [Low Iq Always ON Smart Diode Controller](#)
6. Texas Instruments, [Layout Tips for EMI Reduction in DC/DC Converters](#)

6.1 商标

HotRod is a trademark of Texas Instruments.

All other trademarks are the property of their respective owners.

有关 TI 设计信息和资源的重要通知

德州仪器 (TI) 公司提供的技术、应用或其他设计建议、服务或信息，包括但不限于与评估模块有关的参考设计和材料（总称“TI 资源”），旨在帮助设计人员开发整合了 TI 产品的应用；如果您（个人，或如果是代表贵公司，则为贵公司）以任何方式下载、访问或使用了任何特定的 TI 资源，即表示贵方同意仅为该等目标，按照本通知的条款进行使用。

TI 所提供的 TI 资源，并未扩大或以其他方式修改 TI 对 TI 产品的公开适用的质保及质保免责声明；也未导致 TI 承担任何额外的义务或责任。TI 有权对其 TI 资源进行纠正、增强、改进和其他修改。

您理解并同意，在设计应用时应自行实施独立的分析、评价和判断，且应全权负责并确保应用的安全性，以及您的应用（包括应用中使用的 TI 产品）应符合所有适用的法律法规及其他相关要求。就您的应用声明，您具备制订和实施下列保障措施所需的一切必要专业知识，能够 (1) 预见故障的危险后果，(2) 监视故障及其后果，以及 (3) 降低可能导致危险的故障几率并采取适当措施。您同意，在使用或分发包含 TI 产品的任何应用前，您将彻底测试该等应用和该等应用所用 TI 产品的功能而设计。除特定 TI 资源的公开文档中明确列出的测试外，TI 未进行任何其他测试。

您只有在为开发包含该等 TI 资源所列 TI 产品的应用时，才被授权使用、复制和修改任何相关单项 TI 资源。但并未依据禁止反言原则或其他法律授予您任何 TI 知识产权的任何其他明示或默示的许可，也未授予您 TI 或第三方的任何技术或知识产权的许可，该等许可包括但不限于任何专利权、版权、屏蔽作品权或与使用 TI 产品或服务的任何整合、机器制作、流程相关的其他知识产权。涉及或参考了第三方产品或服务的信息不构成使用此类产品或服务的许可或与其相关的保证或认可。使用 TI 资源可能需要您向第三方获得对该等第三方专利或其他知识产权的许可。

TI 资源系“按原样”提供。TI 兹免除对 TI 资源及其使用作出所有其他明确或默示的保证或陈述，包括但不限于对准确性或完整性、产权保证、无屡发故障保证，以及适销性、适合特定用途和不侵犯任何第三方知识产权的任何默认保证。

TI 不负责任何申索，包括但不限于因组合产品所致或与之有关的申索，也不为您辩护或赔偿，即使该等产品组合已列于 TI 资源或其他地方。对因 TI 资源或其使用引起或与之有关的任何实际的、直接的、特殊的、附带的、间接的、惩罚性的、偶发的、从属或惩戒性损害赔偿，不管 TI 是否获悉可能会产生上述损害赔偿，TI 概不负责。

您同意向 TI 及其代表全额赔偿因您不遵守本通知条款和条件而引起的任何损害、费用、损失和/或责任。

本通知适用于 TI 资源。另有其他条款适用于某些类型的材料、TI 产品和服务的使用和采购。这些条款包括但不限于适用于 TI 的半导体产品 (<http://www.ti.com/sc/docs/stdterms.htm>)、[评估模块](http://www.ti.com/sc/docs/sampters.htm)和样品 (<http://www.ti.com/sc/docs/sampters.htm>) 的标准条款。

邮寄地址：上海市浦东新区世纪大道 1568 号中建大厦 32 楼，邮政编码：200122
Copyright © 2018 德州仪器半导体技术（上海）有限公司